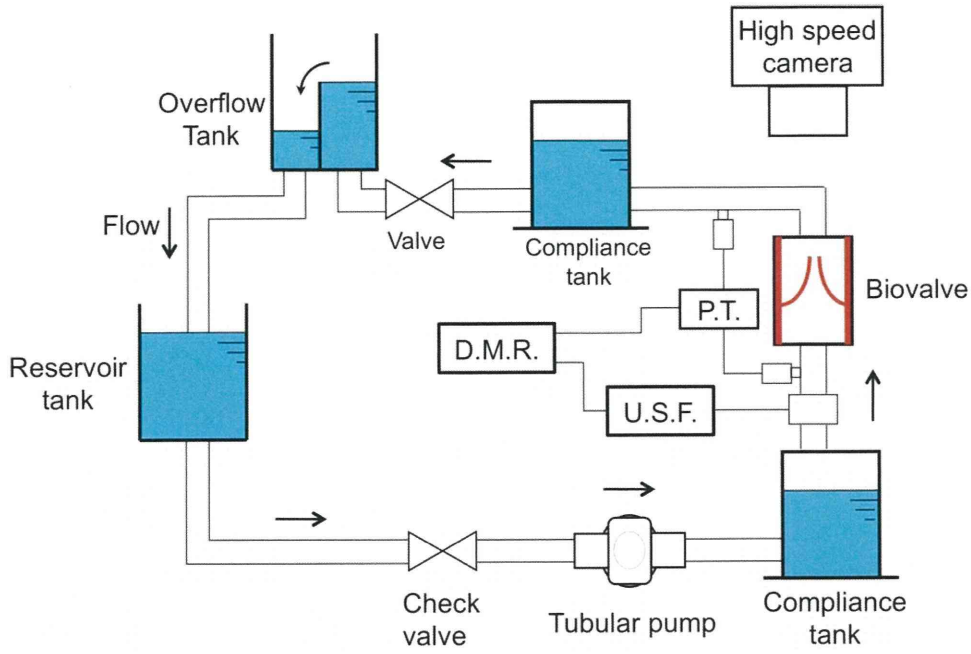

FIGURE 3. A Windkessel-modified pulsatile flow circuit model designed for the evaluation of valve function. The working fluid was 0.9% saline solution, and the stroke volume was 20 mL. [Color figure can be viewed in the online issue, which is available at wileyonlinelibrary.com.]

In vitro valve function

Valve function was examined using a modified Windkessel pulsatile circuit model, which mimicked the systemic arterial system of beagle dogs. The stroke volume was 20 mL, and the working fluid was 0.9% saline solution (Figure 3). The circuit consisted of a tubular pump, compliance tank, overflow tank,

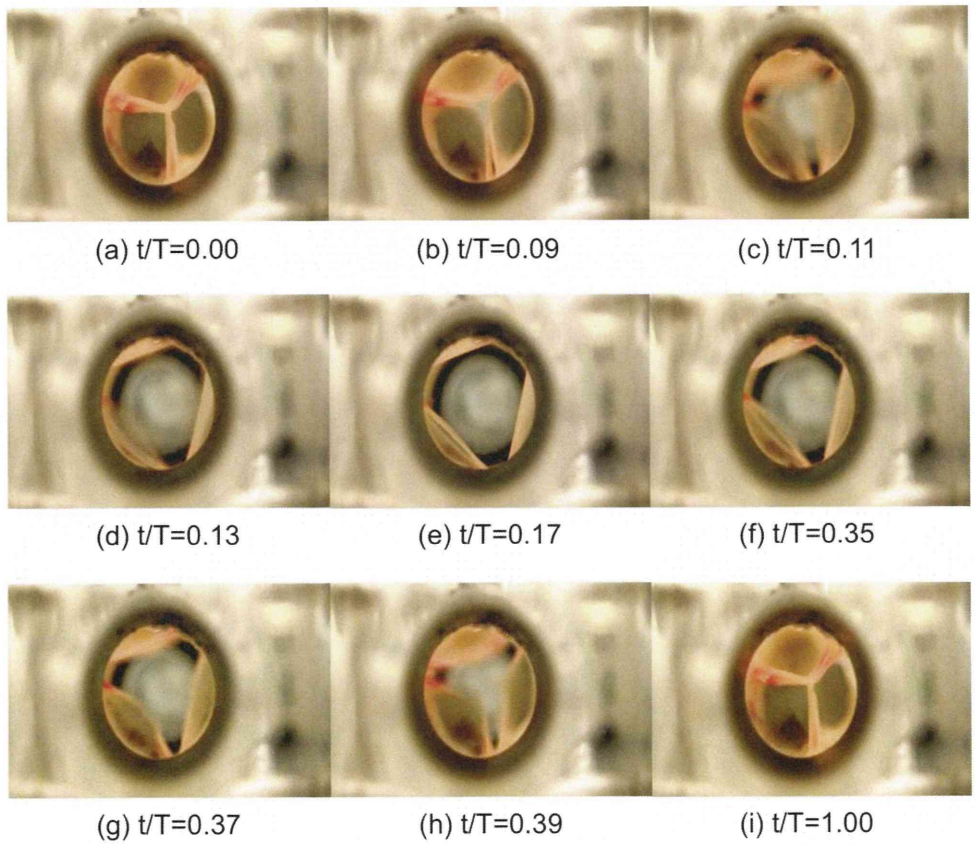

FIGURE 4. Valve movement under pulsatile conditions was recorded with a high-speed video camera at a frequency of 250 frames/s. The pulsatile flow was 40 bpm, and the flow rate was 720 mL/min. [Color figure can be viewed in the online issue, which is available at wileyonlinelibrary.com.]

and reservoir tank. The tubular pump and compliance tank provided pulsatile flow and ensured pressure control, respectively. To provide constant back pressure, an overflow tank was used. The flow rate, left ventricular pressure, and aortic pressure were measured using an electromagnetic flow meter and pressure meter. The pulsatile rate and flow rate were set at 40 bpm and 720 mL/min. Furthermore, the motion of the biovalve leaflet was recorded with a high-speed video camera at a frequency of 250 frames/s. The orifice ratio (OR) was defined as the area ratio of the orifice area (OA) of the valve per unit cross-sectional area of the conduit.

RESULTS

Preparation of the biovalves

The type VI biovalve was prepared by in-body tissue architecture technology using a newly designed silicone mold [Figure 1(F)]. The preparation method was similar to that used for the type V biovalve. As described in our previous study, one end of the convex rod in the type V biovalve had three balls that resembled the three protrusions of the sinus of Valsalva [Figure 1(A)]. Therefore, the shape of the aperture space formed by connecting the two rods was designed such that it was in the open form of a trileaflet. On the other hand, the convex rod of the type VI biovalve had three round sheets at one end [Figure 1(E)], resulting in the formation of the closed form of the trileaflet in the aperture space between the two rods. However, macroscopic observation revealed that there was little difference between the two molds, with the exception that the height of the three protrusions in the type VI biovalve was 2/3rd of that in the type V biovalve [Figure 1(B,F)].

When both type molds were embedded into the subcutaneous pouches of beagles for 4 weeks, the respective biovalves were obtained, and these were completely encapsulated with autologous connective tissues [Figure 1(C,G)]. The implants could also be easily harvested because the developed biovalves and subcutaneous tissue were only connected by very fragile, irregular, and redundant tissues. In the type VI biovalve, thick and homogeneous membranous tissues covered almost the entire outer surface of the mold, even at the top of the three protrusions where the membrane thickness was 275 ± 36 μm [Figure 1(H)]. This was about two times larger than that observed for the type V biovalve [wall thickness; 130 ± 21 μm in Figure 1(D)].

Removal of the rods from both ends of the developed cylindrical-shaped tissue revealed a well-formed tubular-shaped type VI biovalve with three protrusions resembling the sinus of Valsalva. Inside the conduit, three separate membranous leaflets were present, which were connected at the commissure with a small aperture [Figure 2(C)].

In vitro valve function

The movement of the leaflets in a pulsatile flow circuit was examined by videography (Figure 4). The biovalve leaflets closed rapidly and tightly in synchronization with the backward flow in the diastolic phase (Figure 4). Coaptation was optimal. In the transition phase of the flow direction, the valve opened smoothly without flapping or hitting the conduit wall.

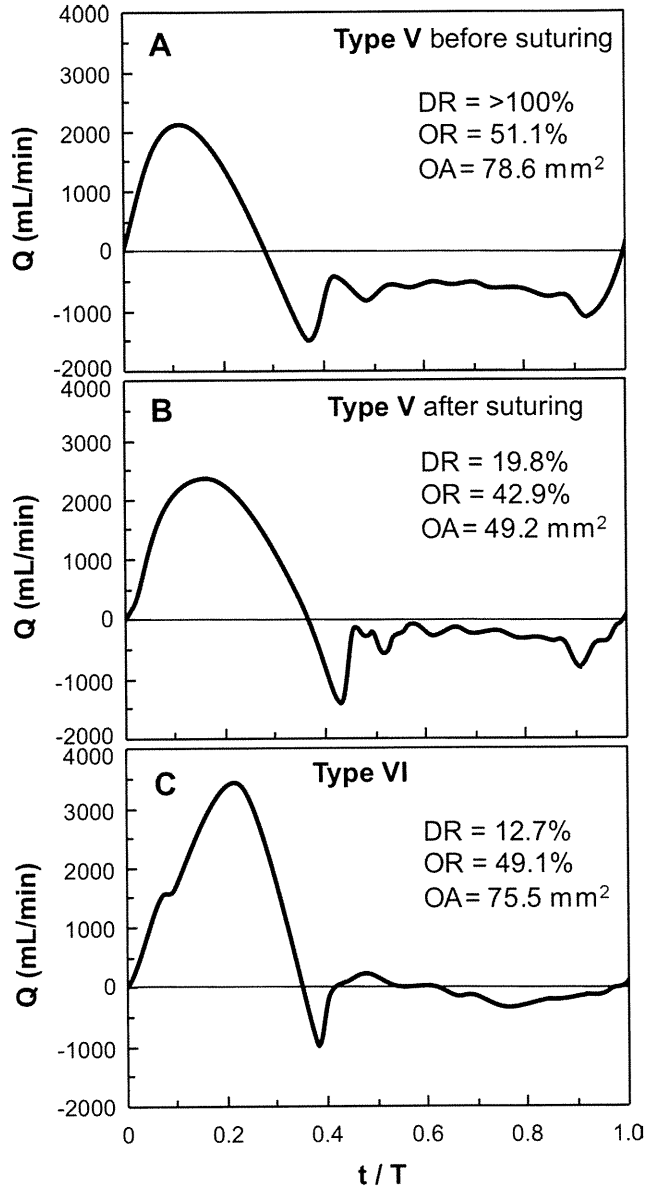

FIGURE 5. Pulsatile flow waveforms in 1 cycle of the type V biovalve before (A) and after suturing at the commissure (B), and in the type VI biovalve (C). DR, OR, and OA in each figure represent the degree of regurgitation, orifice ratio, and orifice area, respectively.

Figure 5 shows a comparison of the flow waveforms of the type VI and type V biovalves before and after suturing the edges of the leaflets at three commissures. These waveforms were ensemble averages of 10 separate sets of experimental data. In all the biovalves, there were little differences between the inflow side pressure and the outflow side pressure in the systolic phase (t/T ranging from 0 to 0.4), indicating that stenosis did not occur in any of the conduits. More than 100% significant regurgitation occurred in the diastolic phase in the type V biovalve [Figure 5(A)]. The biovalve could not work as a valve. However, by eliminating the space between the leaflets at the commissures by

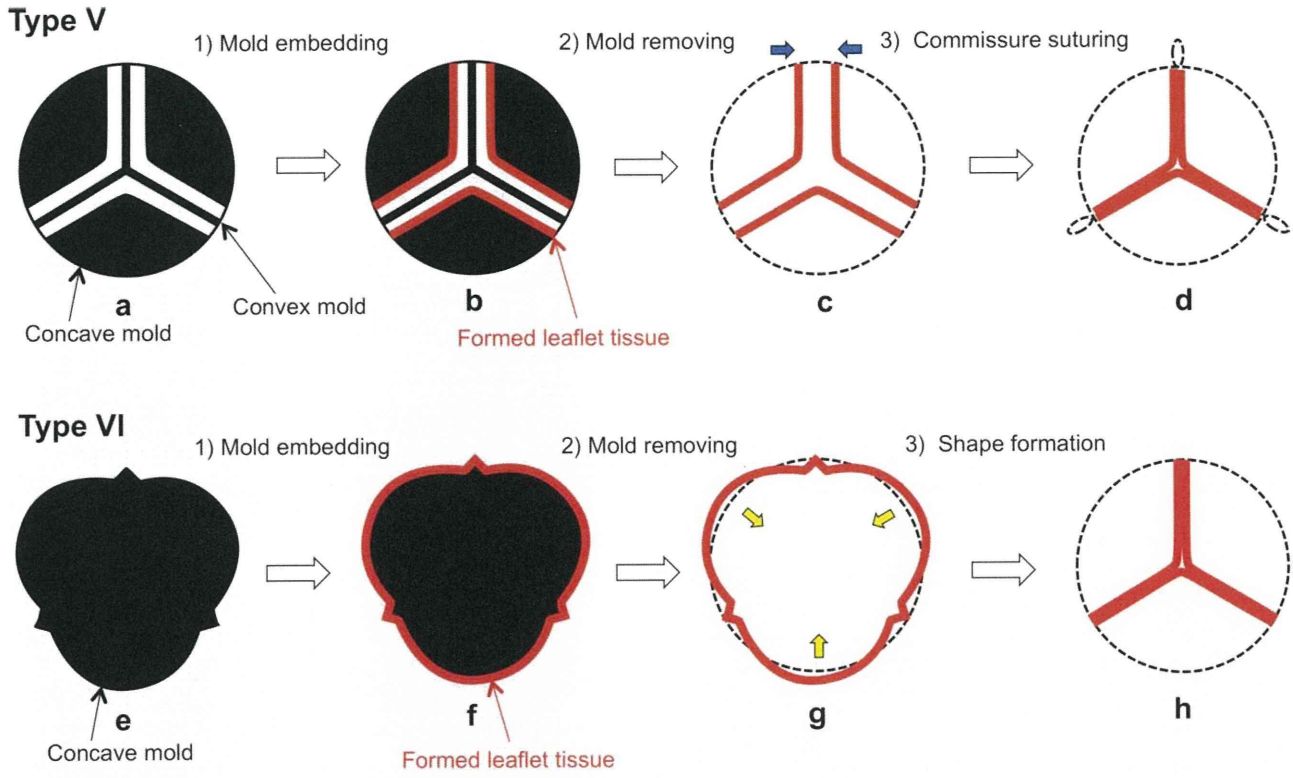

FIGURE 6. The process used to prepare the trileaflets at the circumferential cross-section at the top of the convex rod in both types of biovalves. [Color figure can be viewed in the online issue, which is available at wileyonlinelibrary.com.]

suturing, the degree of regurgitation (DR) was significantly improved to 19.8%, although the OR decreased from 51.1% to 42.9% with a reduction in the OA from 78.6 mm^2 to 49.2 mm^2 [Figure 5(B)]. On the other hand, the type VI biovalve showed a lower regurgitation ratio of 12.7% [Figure 5(C)]. Regurgitation in the diastolic phase was almost completely prevented. In addition, a large OR of 49.1%, and an effective OA of 75.5 mm^2 were obtained.

DISCUSSION

In this study, we developed a biovalve with near perfect valve function by greatly altering the design concept of the mold used to prepare the biovalves. The key difference between the mold devised in this study and earlier molds is that the aperture formed with this mold at the two connecting rods is in the shape of a trileaflet. The preparation process of the type VI biovalve developed in this study is summarized and compared with that of the previous type V biovalve in Figure 6. In the type V biovalve,[19] the circumferential cross-section at the top of the convex rods pointed along the combined three lines [Figure 6 (A)]. Our experience suggests that the aperture between two rods should be at least 1 mm for leaflet formation. Because the thickness of the top of the convex rod was 0.5 mm, the total width of the aperture was 2.5 mm. In addition, whereas subcutaneous embedding the membranous connective tissue was grown for covering the molds with the least area. Therefore, very small leaflet cups were formed within the aperture, resulting in the formation of a closed leaflet [Figure 6 (B)]. Naturally, the wide aperture induced significant regurgitation [Figure 6 (C)] that was ranked as "severe" (DR $\geq$ 50%, OA $\leq$ 0.75 cm^2 in human adult, normal OA = 3–4 cm^2), which is clinically acceptable in the ACC/AHA 2006 guidelines for the management of patients with valvular heart disease.[20] Therefore, prior to the valve replacement experiment, the leaflets at the commissures were sutured to reduce the diameter of the conduit [Figure 6 (D)].

On the other hand, in the type VI biovalve, the convex rod maintained an almost round shape, even at the top [Figure 6 (E)]. Therefore, the leaflets formed an almost circular shape [Figure 6 (F)]. The total length of the leaflets in the circumferential direction was the same in both the completely open form [Figure 6 (G)] and the closed one [Figure 6 (H)]. This resulted in only slight regurgitation that was ranked as "trivial" (DR $\leq$ 30%, OA = 1.1–2.0 cm^2 in human adult) in *in vitro* evaluation with no requirement for post processing [Figure 5(C)]. The occurrence of slight regurgitation might be due to the reduction in the size of the sinus of Valsalva. The vortex flow in the sinus of Valsalva plays an important role in the closure of native semilunar valves and coronary flow.[21] Valves lacking the sinus of Valsalva close only passively due to the backflow of blood.[22] Therefore, in the next generation of biovalves, valves with a compatible thick conduit membrane and of physiological size similar to that of the sinus of Valsalva will be required.

The conditions for *in vitro* valve function were set assuming implantation in beagles of approximate weight 10 kg, in which the average cardiac outflow was approximately

1 L/min, and heart rate was approximately 100 bpm. In the pulsatile flow circuit model shown in Figure 3, 0.9% saline solution was selected as the working fluid to prevent injury in biovalves made of natural tissues. The kinetic viscosity of blood is 4.44×10^{-6} m^2/s, which is approximately four times that of the saline solution (1.00×10^{-6} m^2/s). Therefore, the flow condition in the circuit between the two different fluids, which is defined by the Reynolds number and Womersley number, should be adjusted when evaluating valve function using saline solution. The pulsatile rate and flow rate calculated by the two numbers were 23 bpm and 226 mL/min, respectively. In this study, severe conditions were used (pulsatile rate of 40 bpm, which is approximately two times the normal value and a flow rate of 720 mL/min, which is about three times the normal value) to evaluate high performance. The durability of the biovalve is also of interest to us. Because the biovalve is an engineered tissue, it will have to maintain its function in living bodies, and the living body would be the best environment for testing the biovalve. Therefore, we believe that there is little value in examining the long-term durability of the biovalve in an *in vitro* system. We are planning an *in vivo* implantation study of the biovalve to investigate its long-term durability. This study describes the development of a type VI biovalve using in-body tissue architecture technology. We hope that this type of biovalve may be successfully used for aortic heart valve replacement.

ACKNOWLEDGMENTS

The authors thank Ms. Manami Sone for her technical support.

REFERENCES

1. Vongpatanasin W, Hillis D, Lange RA. Prosthetic heart valves. N Engl J Med 1996;335:407–416.
2. Cannegieter SC, Rosendaal FR, Briët E. Thromboembolic and bleeding complications in patients with mechanical heart valve prostheses. Circulation 1994;89:635–641.
3. Hammermeister KE, Sethi GK, Henderson WG, Oprian C, Kim T, Rahimtoola S. A comparison of outcomes in men 11 years after heart-valve replacement with mechanical valve or bioprosthesis. N Engl J Med 1993;328:1289–1296.
4. Cosgrove DM, Lytle BW, Taylor PC, Camacho MT, Stewart RW, McCarthy PM, Miller DP, Piedmonte MR, Loop FD. The Carpentier-Edwards pericardial aortic valve. Ten-year results. J Thorac Cardiovasc Surg 1995;110:651–662.
5. Mayer JE Jr. Use of homograft conduits for right ventricle to pulmonary connections in the neonatal period. Sem Thorac Cardiovasc Surg 1995;7:130.
6. Watts LK, Duffy P, Field RB, Stafford EG, O'Brien MF. Establishment of a viable homograft cardiac valve bank: A rapid method of determining homograft viability. Ann Thorac Surg 1976;21:230–236.
7. Kirklin JK, Smith D, Novick W, Naftel DC, Kirklin JW, Pacifico AD, Nanda NC, Helmcke FR, Bourge RC. Long-term function of cryopreserved aortic homografts. A ten-year study. J Thorac Cardiovasc Surg 1993;106:154–166.
8. Shinoka T, Ma PX, Shum-Tim D, Breuer CK, Cusick RA, Zund G, Langer R, Vacanti JP, Mayer JE Jr. Tissue-engineered heart valves. Autologous valve leaflet replacement study in a lamb model. Circulation 1996;94:II164–II168.
9. Zund G, Hoerstrup SP, Schoeberlein A, Lachat M, Uhlschmid G, Vogt PR, Turina M. Tissue engineering: A new approach in cardiovascular surgery: Seeding of human fibroblasts followed by human endothelial cells on resorbable mesh. Eur J Cardiothorac Surg 1998;13:160–164.
10. Bader A, Steinhoff G, Strobl K, Schilling T, Brandes G, Mertsching H, Tsilkas D, Froelich J, Haverich A. Engineering of human vascular aortic tissue based on a xenogenetic starter matrix. Transplantation 2000;70:7–14.
11. Elkins RC, Dawson PE, Goldstein S, Walsh SP, Black KS Decellularized human valve allografts. Ann Thorac Surg 2001;71: S428–S432.
12. Hoerstrup SP, Kadner A, Melnitchouk S, Trojan A, Eid K, Tracy J, Sodian R, Visjager JF, Kolb SA, Grunenfelder J, Zund G, Turina MI. Tissue engineering of functional trileaflet heart valves from human marrow stromal cells. Circulation 2002;106: I143–I150.
13. Nakayama Y, Ishibashi-Ueda H, Takamizawa K. In vivo tissue-engineered small-caliber arterial graft prosthesis consisting of autologous tissue (biotube). Cell Transplant 2004;13:439–449.
14. Watanabe T, Kanda K, Ishibashi-Ueda H, Yaku H, Nakayama Y. Autologous small-caliber "biotube" vascular grafts with argatroban loading: A histomorphological examination after implantation to rabbits. J Biomed Mater Res B Appl Biomater 2010;92:236–242.
15. Hayashida K, Kanda K, Yaku H, Ando J, Nakayama Y. Development of an *in vivo* tissue-engineered, autologous heart valve (the biovalve): Preparation of a prototype model. J Thorac Cardiovasc Surg 2007;134:152–159.
16. Hayashida K, Kanda K, Oie T, Okamoto Y, Ishibashi-Ueda H, Onoyama M, Tajikawa T, Ohba K, Yaku H, Nakayama Y. Architecture of an in vivo-tissue engineered autologous conduit "Biovalve". J Biomed Mater Res B Appl Biomater 2008;86:1–8.
17. Nakayama Y, Yamanami M, Yahata Y, Tajikawa T, Ohba K, Watanabe T, Kanda K, Yaku H. Preparation of a completely autologous trileaflet valve-shaped construct by in-body tissue architecture technology. J Biomed Mater Res B Appl Biomater 2009;91: 813–818.
18. Yamanami M, Yahata Y, Tajikawa T, Ohba K, Watanabe T, Kanda K, Yaku H, Nakayama Y. Preparation of *in-vivo* tissue-engineered valved conduit with the sinus of Valsalva (type IV biovalve). J Artif Organs 2010;13:106–112.
19. Yamanami M, Yahata Y, Uechi M, Fujiwara M, Ishibashi-Ueda H, Kanda K, Watanabe T, Tajikawa T, Ohba K, Yaku H, Nakayama Y Development of a completely autologous valved conduit with the sinus of valsalva using in-body tissue architecture technology: A pilot study in pulmonary valve replacement in a beagle model. Circulation 2010;122:S100–S106.
20. Bonow RO, Carabello BA, Chatterjee K, de Leon AC Jr, Faxon DP, Freed MD, Gaasch WH, Lytle BW, Nishimura RA, O'Gara PT, O'Rourke RA, Otto CM, Shah PM, Shanewise JS, Smith SC Jr, Jacobs AK, Adams CD, Anderson JL, Antman EM, Fuster V, Halperin JL, Hiratzka LF, Hunt SA, Lytle BW, Nishimura R, Page RL, Riegel B. ACC/AHA 2006 guidelines for the management of patients with valvular heart disease: A report of the American College of Cardiology/American Heart Association Task Force on Practice Guidelines (writing Committee to Revise the 1998 guidelines for the management of patients with valvular heart disease) developed in collaboration with the Society of Cardiovascular Anesthesiologists endorsed by the Society for Cardiovascular Angiography and Interventions and the Society of Thoracic Surgeons. J Am Coll Cardiol 2006;48:e1–148.
21. Kunzelman KS, Grande KJ, David TE, Cochran RP, Verrier ED. Aortic root and valve relationships. Impact on surgical repair. J Thorac Cardiovasc Surg 1994;107:162–170.
22. Ohta Y, Kikuta Y, Shimooka T, Mitamura Y, Yuhta T, Dohi T. Effect of the sinus of Valsalva on the closing motion of bileaflet prosthetic heart valves. Artif Organs 2000;24:309–312.

Bioconjugate Chemistry

ARTICLE

pubs.acs.org/bc

Thermoresponsive Heparin Bioconjugate as Novel Aqueous Antithrombogenic Coating Material

Yasuhide Nakayama,[*,†,‡] Saori Yamaoka,[†,§] Yasushi Nemoto,[∥] Borovkov Alexey,[†,‡] and Kingo Uchida[§]

[†]Division of Medical Engineering and Materials, National Cerebral and Cardiovascular Center Research Institute

[‡]Biological Chemistry and Biochemical Engineering Course, Graduate School of Chemical Science and Engineering, Hokkaido University

[§]Department of Materials Chemistry, Faculty of Science and Technology, Ryukoku University

[∥]Chemical Products Divison, Development Department, Brigestone Corporation

ABSTRACT: A novel thermoresponsive aqueous antithrombogenic coating material comprising a heparin bioconjugate with a six-branched, star-shaped poly(2-(dimethylaminoethyl)-methacrylate) (6B-PDMAEMA), which has both thermoresponsive and cationic characters, was developed to reduce the thrombogenic potential of blood-contacting materials such as synthetic polymers or tissue-engineered tissues in cardiovascular devices. 6B-PDMAEMA with M_n of ca. 24 kDa was designed as a prototype compound by initiator-transfer agent-terminator (iniferter)-based living radical photopolymerization from hexakis(*N,N*-diethyldithiocarbamylmethyl)benzene. Bioconjugation of heparin with 6B-PDMAEMA occurred as soon as both aqueous solutions were simply mixed to form particles. The particle size at 25 °C was less than several hundred nanometers in diameter under a heparin/6B-PDMAEMA mixing weight ratio of over 2.5. The particles were very stable because of the prevention of hydrolysis of 6B-PDMAEMA in its bioconjugated form. Because the lower critical solution temperature of the bioconjugate ranges from approximately 20 to 36 °C for the formation of microparticles, the coating could be done in an aqueous solution at low temperatures. The excellent adsorptivity and high durability of the coating above 37 °C was demonstrated on silicone and polyethylene films by surface chemical compositional analysis. Blood coagulation was significantly reduced on the bioconjugate-coated surfaces. Therefore, the thermoresponsive bioconjugate developed here appears to satisfy the initial requirements for a biocompatible aqueous coating material.

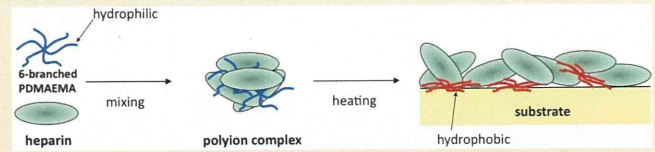

INTRODUCTION

Various surface modification techniques using heparin, which has potent anticoagulant activity when complexed with antithrombin III (ATIII), have been proposed and developed for conferring aniticoagulant properties to the blood-contacting surfaces of extracorporeal[1,2] and implantable devices such as stents[4,5] and catheters. These techniques include surface physical mixing,[6,7] coating with a surfactant−heparin bioconjugate[8,9] or a simple electrostatic self-assembly method,[10,11] surface derivatization through chemical bonding with or without a spacer arm,[12,13] and hydrogel immobilization.[14,15] Among these techniques, coating is one of the most popular ones. However, organic solvents usually used for coating of polymeric materials are difficult to use as a coating material for surface heparinization of natural tissues.

Previously, we designed an aqueous surfactant material for the thermoresponsive surface immobilization of heparin.[8] The material comprised four AB-type blocked branches, each incorporating two different chemical entities—a cationic poly(*N,N*-dimethylaminopropylacrylamide) (PDMAPAAm) block and a thermoresponsive poly(*N*-isopropylacrylamide) (PNIPAM) block. PNIPAM is the most popular thermally sensitive water-soluble nonionic polymer having a low critical solution temperature (LCST) of almost 32 °C.[16,17] Upon mixing the surfactant with heparin in an aqueous medium at room temperature, nanoparticles were produced by formation of heparin bioconjugate. Upon heating the aqueous solution to 37 °C, the particles aggregated and adsorbed on the surface of the biomedical materials or natural polymers by hydrophobic interaction.

Poly(2-(dimethylaminoethyl)methacrylate) (PDMAEMA) is also known as one of the thermoresponsive polymers, and at higher temperatures, the polymer phase separates from the solution by hydrophobic interaction between the polymers as a result of a breakdown in the hydrogen bonding interactions.[18−20] Recent advances in living radical polymerization (LRP)[21,22] and reversible addition−fragmentation transfer (RAFT) polymerization[23−25] allow for the synthesis of PDMAEMA with a tunable polymer chain length and macromolecular architecture, as well as a narrow molecular weight distribution. The solubility of PDMAEMA in an aqueous solution is pH-dependent. At pH 7, PDMAEMA is partially charged (hydrophilic) and partially uncharged (hydrophobic), resulting in an amphiphilic molecule. At lower pH, the polymer becomes more positively charged, and at pH values greater than 8, it becomes mostly uncharged.

Received: June 11, 2010
Revised: December 10, 2010
Published: January 20, 2011

Because of its cationic character,[26] DMAEMA is applied as a nonviral gene delivery vector.[27−29] Thus, PDMAEMA has the unique characteristics of being both cationic and thermoresponsive. However, strangely, there is little found in the biomedical research literature dealing with this dual characteristic of the polymer.

This study reports on the development of a novel surfactant for an aqueous antithrombogenic coating material; it incorporates the advantages of PDMAEMA having the above-mentioned two unique characteristics. It was expected that the cationic character of PDMAEMA will interact with heparin to form heparin bioconjugates, and its thermoresponsive character will enable the surface immobilization of the bioconjugates to biomedical materials. In our previous report,[30] to improve gene transfection efficiency using cationic polymers, we designed a series of branched cationic polymers, linear and 3-, 4-, or 6-branched poly(*N,N*-dimethylaminopropylacrylamide) as a novel high-performance gene carrier called star vector, prepared to have the same molecular weight. The relative gene expression efficiency increased in the degree of branching that may affect the cationic charge density, and the compaction of DNA polyplexes was stabilized on an increase in the branch number. In addition to the evidence, for the effective surface immobilization of heparin, a star-shaped six-branching configuration, which was expected to confer strong multipoint adsorption, was incorporated into the surfactant structure. The precise preparation of the branching was performed by initiator−transfer agent−terminator (iniferter)-based living radical photopolymerization. The surface functionality and a preliminary characterization of the biological activity of the heparin bioconjugate are described.

EXPERIMENTAL SECTION

Materials. Hexakis(bromomethyl)benzene was obtained from Sigma-Aldrich (Milwaukee, WI). Sodium *N,N*-diethyldithiocarbamate, *N*-[2-(dimethylamino)ethyl]methacrylate (DMAEMA) was purchased from Wako Pure Chemical Ind., Ltd. (Osaka, Japan). Other chemical reagents were commercially obtained from Wako Pure Chemical Ind., Ltd. The DMAEMA was distilled under reduced pressure before use in order to remove the stabilizer. The other reagents were purified before use as required.

General Methods. ^{1}H NMR spectra were recorded in deuterium oxide (D_2O) using a 300 MHz NMR spectrometer (Gemini 300; Varian, Palo Alto, CA) at room temperature. Gel permeation chromatography (GPC) analyses using *N,N*-dimethylformamide as a solvent were carried out using an HPLC-8020 instrument (Tosoh, Tokyo, Japan) using Tosoh TSKgel α-3000 and α-5000 columns. The columns were calibrated with narrow weight distribution poly(ethylene glycol) standards (Tosoh). Zeta potentials were measured using a Zetasizer Nano-ZS (Malvern Instrument Ltd., Worcestershire, U.K.).

Synthesis of Hexakis(*N,N*-diethyldithiocarbamyl(poly(*N*-[2-(dimethylamino)ethyl]methacrylate))benzene (6B-PDMAEMA)[30,31]. 6B-PDMAEMA was synthesized by iniferter-based living radical photopolymerization from hexakis(*N,N*-diethyldithiocarbamylmethyl)benzene as a 6-functional iniferter with DMAEMA (Figure 1).

An ethanol solution (100 mL) of hexakis(bromomethyl)-benzene (1.0 g, 1.6 mmol) and sodium *N,N*-diethyldithiocarbamate trihydrate (3.3 g, 14.4 mmol) was stirred for 96 h at room

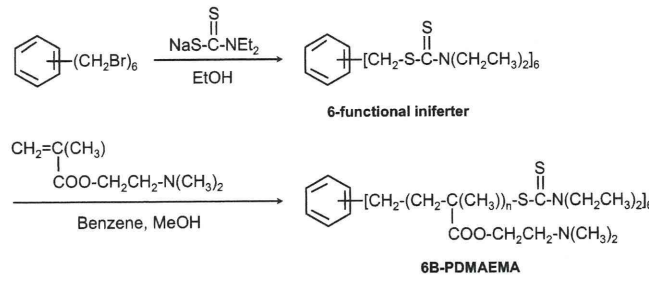

Figure 1. Synthetic route of 6B-PDMAEMA.

temperature. The resulting precipitate was filtered, washed three times with approximately 1 L of methanol, and recrystallized using a chloroform/methanol solution. The yield of hexakis(*N,N*-diethyldithiocarbamylmethyl)benzene (6-functional iniferter) was 1.5 g (yield, 90%). ^{1}H NMR (in chloroform-d_1): δ 1.26−1.31 (m, 36H, $-CH_2-CH_3$), 3.71−3.73 (q, 12H, $-N-CH_2-$), 3.99−4.01 (q, 12H, $-N-CH_2-$), 4.57 (s, 12H, $Ar-CH_2$).

A 6-functional iniferter (44 mg, 42 μmol) was dissolved in approximately 20 mL of chloroform. DMAEMA (8.0 g, 51 mmol) was added to the solution. The total volume of the solution with chloroform increased to 50 mL. The concentrations of the iniferter and monomer were 5.0 mM and 1.0 M, respectively. The mixture was poured into a hard-glass tube (20 × 100 mm; glass thickness, 1 mm), and N_2 gas was bubbled into the glass cell at a flow rate of 2 L/min for 10 min to remove the O_2 gas from the solution. The solution was irradiated for 65 h with a ring-type fluorescent light (FCL30DX, 28 W, NEC Co., light intensity: 2.0 mW/cm^2) under strong stirring. The reaction mixture was concentrated to approximately 10 mL by using a rotary evaporator and poured into 1.0 L of a mixture of diethyl ether and *n*-hexane (1:1 in volume) to obtain a polymeric precipitate. The supernatant solution was removed by decantation. Reprecipitation was carried out 6 times in a chloroform/diethyl ether/*n*-hexane system. The final precipitate was dried under vacuum and dissolved in an adequate quantity of benzene. The resultant benzene solution was filtered with a disposable syringe filter unit having a pore size of 0.22 μm (Mixed Cellulose Ester, Toyo Roshi Ltd., Tokyo, Japan) and freeze−dried for 72 h using a vacuum pump (GCD136X, ULVAC, Tokyo) and a freeze−dryer (FUD 2200, EYELA, Tokyo) to yield 6B-PDMAEMA powder. The molecular weight was determined by gel permeation chromatography (GPC) analysis: M_n = 23 kDa. ^{1}H NMR (in methanol-d_4): δ 0.8−1.2, 1.6−2.0, 2.2−2.4, 2.5−2.7, 4.0−4.2.

Synthesis of Poly(*N*-[2-(dimethylamino)ethyl]methacrylate) (1B-PDMAEMA). No branched, linear PDMAEMA was synthesized by conventional radical polymerization. Into a two-necked reaction vessel were added DMAEMA (3 g, 1.9 × 10^{-2} mol), AIBN (32 mg, 1.9 × 10^{-4} mol), and DMF (10 mL). After stirring at 70 °C for 2 h under N_2 atmosphere, the solvent was removed in vacuo to give a crude product. Reprecipitation was carried out three times in a chroloform/diethyl ether/hexane system. After the last precipitate was dried under reduced pressure, 1B-PDMAEMA was obtained (2.2 g, 73% yield). The molecular weight was determined by gel permeation chromatography (GPC) analysis: M_n = 24 kDa.

Preparation of Heparin Bioconjugate with 6B-PDMAEMA. The heparin bioconjugate was prepared by mixing a PBS (pH 7.4) solution of heparin (1 w/v %) and a PBS solution (pH 7.4) of

6B-PDMAEMA (1 w/v %) at room temperature at a predetermined ratio. The size of the heparin bioconjugate was measured with dynamic light scattering (DLS) using an ELS-8000 system (Otuska Co., Osaka, Japan) equipped with a 10 mW He−Ne laser.

Surface Characterization. The chemical composition of the outermost surface layer was determined by X-ray photoelectron spectroscopy (XPS 3400; Shimadzu Co., Kyoto, Japan) using a magnesium anode (Mg Kα radiation) at room temperature under 5×10^{-6} Torr (10 kV, 20 mA) at a takeoff angle of 90°, where the takeoff angle is defined as the angle between the sample surface and the electron optics of the energy analyzer.

Blood Coagulation Test. Whole blood (ca. 20 mL) was collected from a beagle dog (1 year of age, female, ca. 10 kg) into a conical tube and then immediately dropped (1 mL/sample) on silicone or polyethylene films (thickness: 100 μm, 1×1 cm^2). After incubation at 37 °C for a predetermined time, the samples were rinsed three times with PBS. The gross appearance of the samples was photographed for macroscopic evaluation. This experiment was repeated 4 times.

RESULTS AND DISCUSSION

Preparation and Characterization of Heparin Bioconjugate. The 6B-PDMAEMA, synthesized as a prototype model compound, was star-shaped with 6 branches, had a molecular weight of ca. 23 kDa (ca. 3.8 kDa per branch), and dissolved readily in water at room temperature. The six branches in the 6B-PDMAEMA were designed for multipoint binding to heparin and as highly affective adhesion sites to polymeric or natural tissue surfaces. The control of the chain length was realized by iniferter-based radical photopolymerization.[30,31] In our previous study, polymerization was applied for the development of graft-polymerized surfaces[32,33] or block copolymers as surface coatings, both of which were designed to realize biocompatible surfaces.

When a PBS solution of 6B-PDMAEMA was mixed with a PBS solution of heparin, an increase in the DLS intensity was immediately observed, indicating the formation of heparin/6B-PDMAEMA complexes—the heparin bioconjugate. PDMAEMA has a cationic character due to the cationic nature of the branching dimethylamino groups. In contrast, heparin has an anionic character by virtue of its sulfonic and carboxylic groups. Therefore, the resulting bioconjugates were polyion complexes formed by electrostatic interaction.

The size of the bioconjugates obtained by mixing of equal volumes of a PBS solution of 6B-PDMAEMA and a PBS solution of heparin was 49.9 nm in mean cumulant diameter (Figure 2). The bioconjugate solution was completely precipitated in the physiological temperature range. The equilibrium transmittance and LCST of the bioconjugate solution were 0% and 36.4 °C, respectively, whereas the LCST of 6B-PDMAEMA was 32.0 °C (Figure 3). The increase in LCST after bioconjugation could be caused by the inhibition of the thermoresponsive ability of 6B-PDMAEMA by the binding of the highly hydrophilic heparin. Upon heating the solution at 37 °C, the bioconjugates aggregated to form extremely large particles of approximately 1.7 μm in cumulant diameter (Figure 2). The diameter was notably different from the value (75.2 nm) obtained for a PBS solution of only 6B-PDMAEMA. The molecular size of heparin, which cannot form particles by aggregation, was 2.20 nm at 25 °C and 2.18 nm at 37 °C. Therefore, upon heating to above the

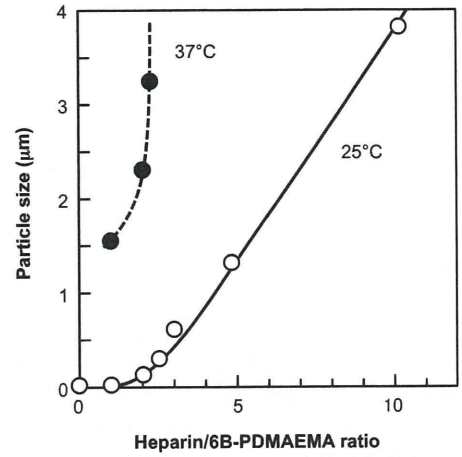

Figure 2. Particle size at 25 or 37 °C of the heparin bioconjugates under different heparin/6B-PDMAEMA ratio.

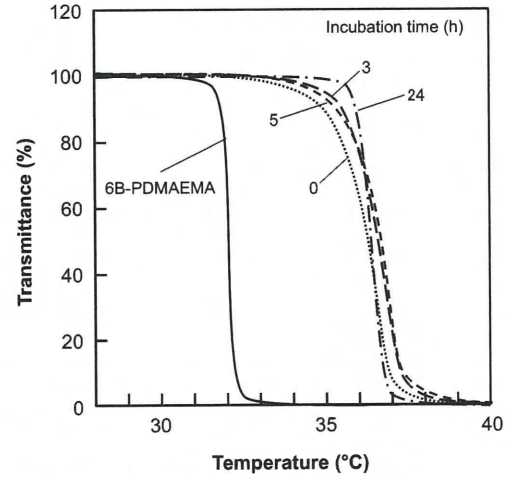

Figure 3. Thermoresponsive change in transmittance of the heparin bioconjugate with heparin/6B-PDMAEMA ratio of 2. Heating rate: 0.5 °C/min.

LCST, 6B-PDMAEMA could be precipitated with the immobilization of heparin. On the other hand, in linear PDMAEMA (1B-PDMAEMA), upon mixing with equal volumes of a PBS solution of heparin the size of the bioconjugates formed was 4.8 nm in mean cumulant diameter, which was one-tenth of that in 6B-PDMAEMA, although both PDMAEMAs had similar molecular weights. In addition, the size of the particles produced upon heating at 37 °C was about half of that in 6B-PDMAEMA (726 nm). The branching structure was effective for the formation of polyion complexes and their aggregation.

The zeta potentials of 6B-PDMAEMA were +7.73 eV at 25 °C and +28.7 eV at 37 °C, whereas there was little change in the values of only heparin by changing temperature (−35.8 eV at 25 °C and −36.2 eV at 37 °C). On the other hand, in the heparin bioconjugates, negative charge increased significantly after heating over LCST (−18.4 eV at 25 °C and −26.2 eV at 37 °C from mixture of heparin/6B-PDMAEMA (1:1)). Increase of cationic charge in 6B-PDMAEMA and anionic charge in the bioconjugates by heating may be due to compaction of the particles by hydrophobic interaction occurred in 6B-PDMAEMA.

dx.doi.org/10.1021/bc100267z |Bioconjugate Chem. 2011, 22, 193–199

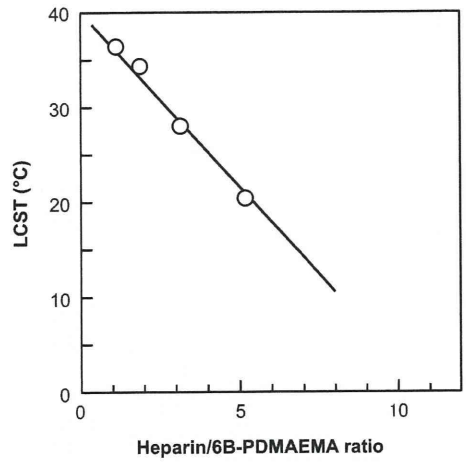

Figure 4. LCST of the heparin bioconjugates under different heparin/6B-PDMAEMA ratios.

With an increase in the amount of heparin in the composition of the heparin bioconjugates, LCST decreased linearly (Figure 4), but the particle size at 25 °C increased significantly (Figure 2). All bioconjugates obtained under a heparin/6B-PDMAEMA ratio of 1.0 converted microparticles by incubation at 37 °C. For Figure 4, the LCST of the bioconjugates decreased with an increase in the content of hydrophilic heparin. This phenomenon seems paradoxical. In general, the LCST increases with an increase of hydrophilic species. In Figure 2, the particle size of the bioconjugates increased significantly with an increase in heparin ratio under the same total concentration. This indicates that PDMAEMA could bind a lot of heparin to form larger-sized bioconjugate particles. It is considered that the larger the particles are, the easier it is to aggregate with each other by hydrophobic interaction upon heating. At described in the Introduction, at higher temperatures, PDMAEMA phase separates from the solution by hydrophobic interaction between the polymers as a result of a breakdown in the hydrogen bonding interactions.[18−20] Therefore, the hydrophilic character of PDMAEMA is converted to a hydrophobic one. Such thermally induced hydrophobicity leads to aggregation of PDMAEMA. Since large-sized bioconjugates could easily aggregate with each other by thermally induced hydrophobic interaction, the LCST decreased for a high heparin/6B-PDMAEMA ratio.

For DMAEMA, the ester in DMAEMA is rather unstable toward hydrolysis (at pH 7.4 and 37 °C, $t_{1/2}$ = 17 h).[34] However, after polymerization the ester groups in the PDMAEMA polymer are quite insensitive toward hydrolysis, even under more extreme conditions (80 °C, pH 1 and 7).[35] Actually, there was little change in the LCST of 1B-PDMAEMA under incubation at 25 °C for 24 h (Figure 5). On the other hand, for 6B-PDMAEMA a time-dependent increase in LCST from 32.0 to 36.5 °C after incubation at 25 °C for 24 h was observed (Figure 5). The branching form may induce hydrolysis. In contrast, there was little change in LCST for the bioconjugate form at 25 °C for 24 h (Figure 3), and the hydrolysis of 6B-PDMAEMA was prevented in the bioconjugation form. Therefore, the bioconjugates were very stable, even under incubation at 37 °C (Figure 6). The particle size of the bioconjugates for a heparin/6B-PDMAEMA ratio of 2 was about 130 nm for 24 h.

Adhesivity of the Bioconjugate. Silicone (Si) and polyethylene (PE) surfaces, both of which are widely used as materials for medical devices, were coated with a PBS solution

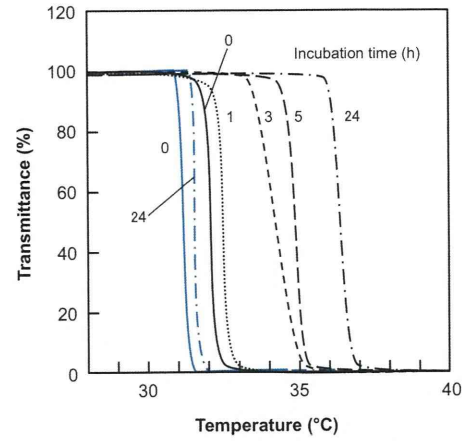

Figure 5. Thermoresponsive change in transmittance of 6B-PDMAEMA (black lines) and 1B-PDMAEMA (blue lines). Heating rate: 0.5 °C/min.

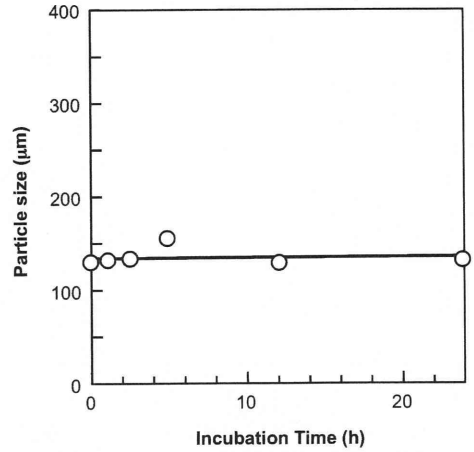

Figure 6. Particle size of the heparin bioconjugate from heparin/6B-PDMAEMA ratio of 2.

of 6B-PDMAEMA or heparin bioconjugates, subsequently air-dried, and then washed with water at 4 or 40 °C. After coating with 6B-PDMAEMA, N_{1s} signals in the XPS spectra mainly originated from dimethylamino groups in the side chains of the 6B-PDMAEMA and were detected on both surfaces. The chemical compositional changes obtained from the XPS spectra are summarized in Table 1. The N/C elemental ratio, determined from peak areas of the C_{1s} and N_{1s}, was 0.12 on both surfaces, which is very close to the theoretical ratio of 6B-PDMAEMA (0.13). The S_{2p} signal originating from the dithiocarbamate group at the terminus of the polymer chains was not detected because it was below the detection limit. In this case, the theoretical S/C elemental ratio, determined from peak areas of the C_{1s} and S_{2p}, was less than 0.01. The N/C ratio was maintained after washing with water at 40 °C, but it was reduced by half after washing at 0 °C. Therefore, 6B-PDMAEMA could immobilize thermally on both polymeric surfaces to prevent delamination at 40 °C, because both polymers have less charge character but are hydrophobic.

On the other hand, upon coating heparin bioconjugate on the Si or PE surfaces, a new S_{2p} signal in addition to the N_{1s} one was detected. The obtained N/C and S/C elemental ratios ranged from 0.07 to 0.12 and from 0.03 to 0.04, respectively. There was

little difference in the ratios after washing with water at 40 °C. However, a small decrease in the ratios was observed after washing with water at 0 °C. The bioconjugate could immobilize strongly compared to the polymer. Interestingly, the bioconjugate with the high heparin content (mixing ratio of heparin/6B-PDMAEMA = 2) could also immobilize in a similar way on both surfaces. On the basis of these observations, it is considered that the heparin bioconjugate displays a strong affinity for the silicone and PE surfaces.

Table 1. Surface Chemical Composition Change of the PE and Si Films before and after Coating of the Heparin Bioconjugate

surface	elemental ratio[b] N/C	S/C
Si[a]	0 (0)	0 (0)
coating with 6B-PDMAEMA	0.12 (0.13)	0 (0)
after washing at 40 °C	0.11	0
after washing at 4 °C	0.05	0
coating with bioconjugate (heparin/polymer = 1)	0.07	0.04
after washing at 40 °C	0.08	0.04
after washing at 4 °C	0.07	0.04
coating with bioconjugate (heparin/polymer = 2)	0.09	0.03
after washing at 40 °C	0.08	0.03
after washing at 4 °C	0.07	0.02
PE[a]	0 (0)	0 (0)
coating with 6B-PDMAEMA	0.12 (0.13)	0 (0)
after washing at 40 °C	0.12	0
after washing at 4 °C	0.06	0
coating with bioconjugate (heparin/polymer = 2)[b]	0.12	0.04
after washing at 40 °C	0.10	0.05
after washing at 4 °C	0.07	0.01
heparin	0.06 (0.08)	0.08 (0.07)

[a] PE: polyethylene. Si: silicone. [b] Determined by electron spectroscopy for chemical analysis.

It is considered that surface modification by a simple coating procedure with heparin bioconjugate can be applied to almost all polymeric medical devices, for example, extracorporeal circulation, in the reduction of the systemic inflammatory response during cardiopulmonary bypass. The coating, which can be applied in the form of an aqueous solution with no risk of damage to the device surface, will be particularly useful for drug-eluting stents (DESs), which have become the most effective devices in interventional treatment for coronary artery disease.

In our previous study,[8] we demonstrated that star-shaped PDMAPAAm-PNIPAM block copolymer was designed for the preparation of heparin bioconjugates and subsequently their surface immobilization on polymeric or natural tissue surfaces. PDMAPAAm had cationic blocks for heparin bioconjugation and PNIPAM blocks for thermoresponsive surface immobilization of the produced bioconjugates. For adequate surface immobilization, the chain length of PNIPAM should be twice as long as the PDMAPAAm chain length and the amount of the polymer double that of heparin. However, for the 6B-PDMAEMA developed here, only half the heparin was needed for the surface immobilization. Therefore, the newly developed material is four times more effective in terms of weight than the previous block copolymer, inducing the exposure of heparin at the outermost layer of the bioconjugate-coated surface.

Antithrombic Activity. The polymeric samples were subjected to whole blood coagulation tests. The degree of coagulation of beagle whole blood was preliminarily evaluated on a silicone and a PE film surface with and without a coating of the heparin bioconjugate. Figure 7 shows photographs of the time-dependent changes in blood coagulation. As expected, there was no blood coagulation on the coated surfaces for up to 30 min, whereas blood gradually coagulated on both of the nontreated polymeric surfaces. A potent anticoagulant property was therefore obtained by heparin surface fixation. The multipoint binding of 6B-PDMAEMA did not diminish the anticoagulant activity of heparin.

Since heparin bioconjugate may be applied to biopolymers such as collagen film and natural tissues, it could contribute to enhancing the reliability of implants involving blood-contacting

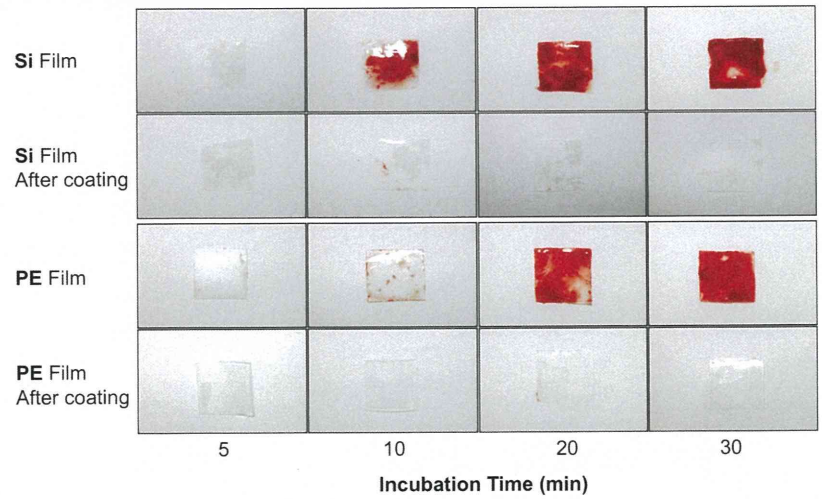

Figure 7. Photographs of silicone (Si) or polyethylene (PE) films before and after heparin bioconjugate coating, on which whole blood was applied to all films, followed by rinsing with a saline solution at 37 °C after a predetermined period of incubation at 37 °C.

dx.doi.org/10.1021/bc100267z |*Bioconjugate Chem.* 2011, 22, 193–199

tissues; for example, it could be useful in a bypass operation during which injured coronary arteries are replaced with homografts. Therefore, our coating material will also undoubtedly be effective for implanting recently developed tissue-engineered tissues or organs with the requisite antithrombogenic properties, which are expected to be the next generation of implantable materials, designed to overcome contemporary clinical difficulties.

In general, PDMAEMA had hydrolysis characteristics in the nonbioconjugate form, also as observed in Figure 5. Therefore, if heparin could be released completely from the heparin bioconjugate immobilized on the blood-contacting surface of medical devices, the remaining cationic surface may convert to an anionic surface by hydrolysis. The anionic surface is more blood-compatible than the cationic one. Therefore, it is expected that the heparin bioconjugate surface will guarantee long-term highly reliable antithrombogenicity.

CONCLUSION

By taking advantage of the cationic and thermoresponsive characteristics of PDMAEMA, a novel heparin bioconjugate was developed for a highly effective heparin surface immobilization material. The heparin bioconjugate was easily prepared by simple mixing of heparin and newly designed 6B-PDMAEMA as a surfactant in aqueous media. Even though the developed material was primarily designed as a prototype model, it appeared to meet the initial requirements for a biocompatible aqueous coating material. Our future research will initially be directed toward the establishment of the molecular weight and the optimization of the surfactant polymer/heparin mixing ratio. We will then proceed to verify the long-term in vivo biocompatible performance, including blood compatibility and toxicological safety, of the heparin bioconjugate. The surface immobilization method developed here will be applied to natural tissue or biopolymer surface as aqueous coating and to the surface immobilization of other anionic biopolymers, including peptides, proteins, RNAs, and DNAs, as demonstrated in our previous studies, such as that on the deposition transfection method.

AUTHOR INFORMATION

Corresponding Author

*To whom correspondence should be addressed. Department of Bioengineering, Advanced Medical Engineering Center, National Cardiovascular Center Research Institute, 5-7-1 Fujishiro-dai, Suita, Osaka 565-8565, Japan. Telephone: (+81) 6-6833-5012 (ex. 2624). Fax: (+81) 6-6872-8090. E-mail: nakayama@ri.ncvc.go.jp.

REFERENCES

(1) Nishinaka, T., Tatsumi, E., Katagiri, N., Ohnishi, H., Mizuno, T., Shioya, K., Tsukiya, T., Homma, A., Kashiwabara, S., Tanaka, H., Sato, M., and Taenaka, Y. (2007) Up to 151 days of continuous animal perfusion with trivial heparin infusion by the application of a long-term durable antithrombogenic coating to a combination of a seal-less centrifugal pump and a diffusion membrane oxygenator. *J. Artif. Organs 10*, 240–244.

(2) Wendel, H. P., and Ziemer, G. (1999) Coating-techniques to improve the hemocompatibility of artificial devices used for extracorporeal circulation. *Eur. J. Cardiothorac. Surg. 16*, 342–350.

(3) Nakayama, Y., Nishi, S., and Ishibashi-Ueda, H. (2003) Fabrication of drug-eluting covered stents with micropores and differential coating of heparin and FK506. *Cardiovasc. Radiat. Med. 4*, 77–82.

(4) Yang., Z., Wang, J., Luo, R., Maitz, M. F., Jing, F., Sun, H., and Huang, N. (2010) The covalent immobilization of heparin to pulsed-plasma polymeric allylamine films on 316L stainless steel and the resulting effects on hemocompatibility. *Biomaterials 31*, 2072–22083.

(5) Aldenhoff, Y. B., Hanssen, J. H., Knetsch, M. L., and Koole, L. H. (2007) Thrombus formation at the surface of guide-wire models: effects of heparin-releasing or heparin-exposing surface coatings. *J. Vasc. Interv. Radiol. 18*, 419–425.

(6) Lin, J. Y., Nojiri, C., Okano, T., and Kim, S. W. (1987) Minimum heparin release rate for nonthrombogenicity. *ASAIO Trans. 33*, 602–605.

(7) Goosen, M. F., and Sefton, M. V. (1979) Heparinized styrene-butadiene-styrene elastomers. *J. Biomed. Mater. Res. 13*, 347–364.

(8) Nakayama, Y., Okahashi, R., Iwai, R., and Uchida, K. (2007) Heparin bioconjugate with a thermoresponsive cationic branched polymer: a novel aqueous antithrombogenic coating material. *Langmuir 23*, 8206–8211.

(9) Gutowska, A., Bae, Y. H., Jacobs, H., Mohammad, F., Mix, D., Feijen, J., and Kim, S. W. (1995) Heparin release from thermosensitive polymer coatings: in vivo studies. *J. Biomed. Mater. Res. 29*, 811–821.

(10) Liu, L., Guo, S., Chang, J., Ning, C., Dong, C., and Yan, D. (2008) Surface modification of polycaprolactone membrane via layer-by-layer deposition for promoting blood compatibility. *J. Biomed. Mater. Res., Sect. B 87*, 244–250.

(11) Barbucc, R., Magnani, A., Albanese, A., and Tempesti, F. (1991) Heparinized polyurethane surface through ionic bonding of heparin. *Int. J. Artif. Organs 14*, 499–507.

(12) Olander, B., Wirsén, A., and Albertsson, A. C. (2003) Silicone elastomer surface functionalized with primary amines and subsequently coupled with heparin. *Biomacromolecules 4*, 145–148.

(13) Marconi, W., Benvenuti, F., and Piozzi, A. (1997) Covalent bonding of heparin to a vinyl copolymer for biomedical applications. *Biomaterials 18*, 885–890.

(14) Nakayama, Y., and Matsuda, T. (1993) Photo induced surface heparin immobilization. *ASAIO J. 39*, M754–M757.

(15) Halstenberg, S., Panitch, A., Rizzi, S., Hall, H., and Hubbell, J. A. (2002) Biologically engineered protein-graft-poly(ethylene glycol) hydrogels: a cell adhesive and plasmin-degradable biosynthetic material for tissue repair. *Biomacromolecules 3*, 710–723.

(16) Miura, M., Cole, C. A., Monji, N., and Hoffman, A. S. (1994) Temperature-dependent absorption/desorption behavior of lower critical solution temperature (LCST) polymers on various substrates. *J. Biomater. Sci. Polym. Ed. 5*, 555–568.

(17) Heskins, M., and Guillet, J. E. (1968) Solution Properties of Poly(N-isopropylacrylamide. *J. Macromol. Sci., Chem. 2*, 1441–1455.

(18) Xue, J., Chen, L., Wang, H. L., Zhang, Z. B., Zhu, X. L., Kang, E. T., and Neoh, K. G. (2008) Stimuli-responsive multifunctional membranes of controllable morphology from poly(vinylidene fluoride)-graft-poly[2-(N,N-dimethylamino)ethyl methacrylate] prepared via atom transfer radical polymerization. *Langmuir 24*, 14151–14158.

(19) Matsumoto, T., Bakamae, K., Okubo, M., Sue, M., Shimao, M., and Komura, M. (1974) Flocculation of hedoro by temperature-sensitive flocculant. *Kobunshi Ronbunshu 31*, 669–675.

(20) Jana, S., Rannard, S. P., and Cooper, A. I. (2007) Structure-LCST relationships for end-functionalized water-soluble polymers: an "accelerated" approach to phase behaviour studies. *Chem. Commun. 28*, 2962–2964.

(21) Xue, J., Chen, L., Wang, H. L., Zhang, Z. B., Zhu, X. L., Kang, E. T., and Neoh, K. G. (2008) Stimuli-responsive multifunctional membranes of controllable morphology from poly(vinylidene fluoride)-graft-poly[2-(N,N-dimethylamino)ethyl methacrylate] prepared via atom transfer radical polymerization. *Langmuir* [Epub ahead of print].

(22) Jiang, X., Lok, M. C., and Hennink, W. E. (2007) Degradable-brushed pHEMA-pDMAEMA synthesized via ATRP and click chemistry for gene delivery. *Bioconjugate Chem. 18*, 2077–2084.

(23) You, Y. Z., Zhou, Q. H., Manickam, D. S., Wan, L., Mao, G. Z., and Oupický, D. (2007) Dually responsive multiblock copolymers via

RAFT polymerization: Synthesis of temperature- and redox-responsive copolymers of PNIPAM and PDMAEMA. *Macromolecules 40*, 8617–8624.

(24) Roy, D., Knapp, J. S., Guthrie, J. T., and Perrier, S. (2008) Antibacterial cellulose fiber via RAFT surface graft polymerization. *Biomacromolecules 9*, 91–99.

(25) You, Y. Z., Manickam, D. S., Zhou, Q. H., and Oupický, D. (2007) Reducible poly(2-dimethylaminoethyl methacrylate): synthesis, cytotoxicity, and gene delivery activity. *J. Controlled Release 122*, 217–225.

(26) Liu, G., Wu, D., Ma, C., Zhang, G., Wang, H., and Yang, S. (2007) Insight into the origin of the thermosensitivity of poly-[2-(dimethylamino)ethyl methacrylate]. *ChemPhysChem 8*, 2254–2259.

(27) Dai, F., Sun, P., Liu, Y., and Liu, W. (2010) Redox-cleavable star cationic PDMAEMA by arm-first approach of ATRP as a nonviral vector for gene delivery. *Biomaterials 31*, 559–569.

(28) Layman, J. M., Ramirez, S. M., Green, M. D., and Long, T. E. (2009) Influence of polycation molecular weight on poly(2-dimethylaminoethyl methacrylate)-mediated DNA delivery in vitro. *Biomacromolecules 10*, 1244–1252.

(29) Xu, F. J., Zhang, Z. X., Ping, Y., Li, J., Kang, E. T., and Neoh, K. G. (2009) Star-shaped cationic polymers by atom transfer radical polymerization from beta-cyclodextrin cores for nonviral gene delivery. *Biomacromolecules 10*, 285–293.

(30) Nakayama, Y., Masuda, T., Nagaishi., M., Hayashi, M., Ohira, M., and Harada-Shiba, M. (2005) High performance gene delivery polymeric vector: nano-structured cationic star polymers (star vectors). *Curr. Drug Delivery 2*, 53–57.

(31) Nakayama, Y., Kakei, C., Ishikawa, A., Zhou, Y. M., Nemoto, Y., and Uchida, K. (2007) Synthesis and in vitro evaluation of novel star-shaped block copolymers (blocked star vectors) for efficient gene delivery. *Bioconjugate Chem. 18*, 2037–2044.

(32) Brodbeck, W. G., Patel, J., Voskerician, G., Christenson, E., Shive, M. S., Nakayama, Y., Matsuda, T., Ziats, N. P., and Anderson, J. M. (2002) Biomaterial adherent macrophage apoptosis is increased by hydrophilic and anionic substrates in vivo. *Proc. Natl. Acad. Sci. U.S.A. 99*, 10287–10292.

(33) Nakayama, Y., and Matsuda, T. (1996) Surface macromolecular architectural designs using photo-graft copolymerization based on photochemistry of benzyl N,N-diethyldithiocarbamate. *Macromolecules 29*, 8622–8630.

(34) The chemical database of DMAEMA reported from Chemicals Evaluation and Research Institute, Japan.

(35) van der Wetering, P., Zuidam, N. J., van Steenbergen, M. J., van der Houwen, O. A. G. J., Underberg W. J. M., and Hennink, W. E. (1998) A mechanistic study of the hydrolytic stability of poly(2-(dimethylamino)ethyl methacrylate), *Macromolecules 31*, 8063−8068.

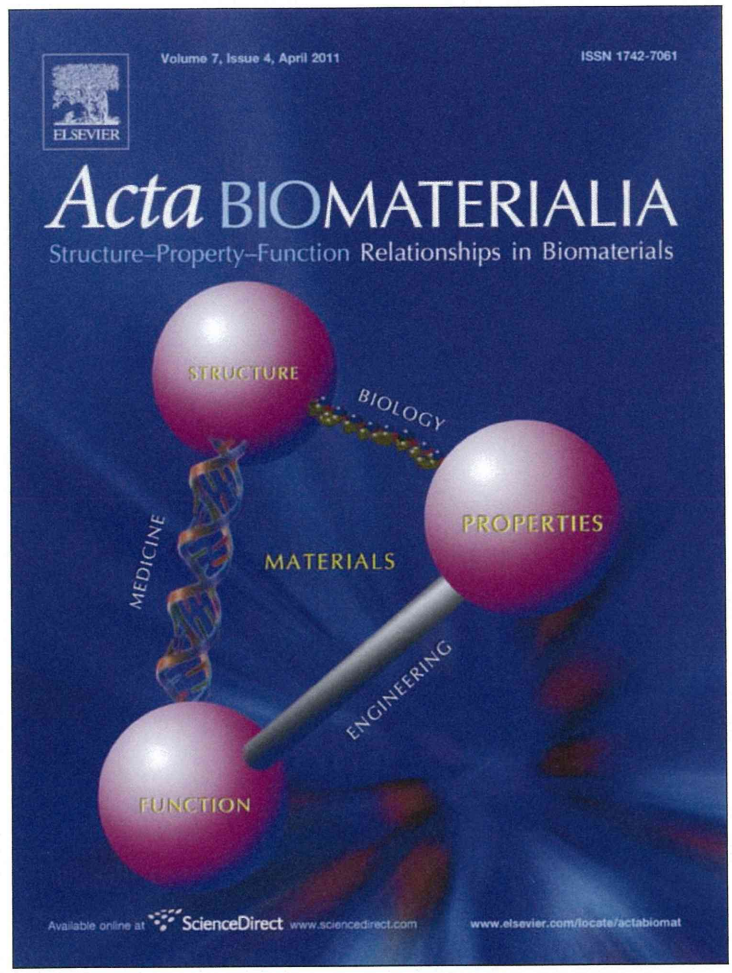

Acta Biomaterialia 7 (2011) 1496–1503

Contents lists available at ScienceDirect

Acta Biomaterialia

journal homepage: www.elsevier.com/locate/actabiomat

Preparation of well-defined poly(ether–ester) macromers: Photogelation and biodegradability

Yasuhide Nakayama [a,*], Kanna Okuda [a], Keiichi Takamizawa [a], Atsuyoshi Nakayama [b]

[a] Division of Medical Engineering and Materials, National Cerebral and Cardiovascular Center Research Institute, 5-7-1 Fujishiro-dai, Suita, Osaka 565-8565, Japan
[b] Bio-based Polymers Collaborative Research Team, AIST Kansai Collaboration Center, 1-8-31 Midorigaoka, Ikeda, Osaka 563-8577, Japan

ARTICLE INFO

Article history:
Received 27 July 2010
Received in revised form 12 November 2010
Accepted 17 November 2010
Available online 21 November 2010

Keywords:
Biodegradation
Poly(ether–ester)
Macromer
Photo-crosslinking
Hydrogel

ABSTRACT

Two series of poly(ether–ester)-based bis-functional macromers terminated with acrylate groups and a well-defined number of ester bonds were synthesized. One series had a chain of 1, 3 or 5 ester bonds at both ends of the central poly(ethylene glycol) block (molecular weight, about 1000), while the other had an alternating structure of oligo(ethylene glycol) each of them linked to two ester bonds, in which 6 or 10 ester bonds were incorporated equally in the macromer molecules and the total molecular weight was adjusted by about 1000. Irradiation of all poly(ether–ester) macromers mixed with camphorquinone resulted in the formation of gels. Gel yield increased and hydrophilic properties of the gels produced decreased with irradiation time. The elastic modulus of the gels decreased with the number of ester bonds. Upon incubation in a PBS solution (pH 8.04), all gels were gradually degraded with time. At 3 weeks of incubation, the degradation ratio increased linearly with the number of ester bonds per unit of molecular weight of the macromers. The order of in vivo degradation rates determined from weight loss was similar to that of the in vitro study. Thus, these poly(ether–ester) macromers may be useful for biodegradable biomaterials or tissue engineering scaffolds.

1. Introduction

Hydrogels are swollen crosslinked polymeric materials that are known to possess excellent biocompatibility due to their high water content, and have hence been used in various biomedical and pharmaceutical applications. These include tissue-engineered scaffolds [1,2], wound-dressing materials [3], tissue adhesive glues [4] and controlled drug delivery devices [5]. In these applications, it is desirable for the hydrogels to be biodegraded or bioresorbed in accordance with the wound healing rate or to control the drug-releasing rate. Accordingly, biodegradable polymers for the matrix of hydrogel poly(anhydride)s [6], poly(ester)s [7] and poly(phosphazene)s [8] that produce non-toxic degradation products are currently being developed in the biomedical area.

Since polyethylene glycol (PEG) is non-toxic and nonimmunogenic, it is excreted rapidly out of the body when it is below a certain molecular weight without inducing immune or allergic reactions. PEG is also soluble in water and other organic solvents at physiological temperatures. To utilize these unique properties of PEG, its application to a wide range of fields, including medicine, pharmacology and engineering, is being evaluated [9,10]. For example, introduction of PEG chains into protein has been evaluated to determine if this can reduce the immunogenicity [11] and solubilization of proteins in organic solvents [12], and to improve physicochemical stability [13]. Fixation of PEG chains on the surface of blood-contacting devices has been attempted to prevent protein adsorption [14] and cell adhesion [15]. PEG is also used as a gel matrix for drug delivery [16]. Moreover, because PEG macromers form hydrogels under suitable conditions, the possibility of their use as in situ-gelating wound-dressing materials is being evaluated [17]. However, since it is extremely difficult to degrade the ether bonds that constitute PEG, hydrogels consisting exclusively of PEG chains are barely degraded in the body. If PEG can be made biodegradable, surgical removal of a wound dressing material or a matrix for drug delivery implanted in the body will become unnecessary, and the rate of drug release can be controlled.

Conversely, aliphatic polyester [18] is a representative degradable macromolecular material, and polylactides [19] and poly(ε-caprolactone) [20,21] obtained by ring-opening polymerization have already been put on the market. Aliphatic polyesters synthesized by polycondensation have also been evaluated. All of these efforts have demonstrated the effectiveness of incorporation of readily hydrolyzable ester bonds for increasing the biodegradability of a material. In PEG gel, introduction of ester bonds has also been evaluated to determine if it can confer degradability to the gel. For example, synthesis of biodegradable copolyester ether by ring-opening copolymerization of anhydrous succinic acid and oxirane, gel formation by condensation of PEG carboxylated at both terminals and

* Corresponding author. Tel.: +81 6 6833 5004x2624; fax: +81 6 6872 8090.
E-mail address: nakayama@ri.ncvc.go.jp (Y. Nakayama).

1742-7061/$ - see front matter © 2010 Acta Materialia Inc. Published by Elsevier Ltd. All rights reserved.
doi:10.1016/j.actbio.2010.11.023

polyhydroxylated PEG, and gel formation using macromers in which oligo α-hydroxylic acid, D,L-lactate, and glycolic acid were introduced at both ends of the PEG have been reported [22].

The photopolymerization techniques required to synthesize crosslinked degradable polymers were developed for biomedical applications. Sawhney et al. [22] developed PEG–co-poly(α-hydroxy acid) diacrylate macromers to prevent postoperative adhesions or restenosis. Elisseeff et al. [23] also used the photopolymerization technique to synthesize crosslinked polymers based on poly(L-lactic acid-co-aspartic acid). Photopolymerized polyanhydrides were synthesized by Anseth et al. [24]. Kim et al. [25] developed crosslinked poly(ether–ester) networks formed by UV photoirraditation. All of these materials have the potential for use as biodegradable lubricants for coating various medical products to replace the existing nondegradable silicone-based materials that are currently in use.

The photo-induced gelation technique has several advantages over other cross-linking techniques, such as fast curing rates at room temperature or 37 °C, spatial and temporal control of the polymerization, the ability to place the gel in vivo without surgical intervention, and minimal heat production [26]. Previously, we developed photocurable gelatins that were partially derivatized with photo-induced radical-generating groups such as UV-reactive benzophenone and visible light-reactive xanthene dyes (e.g. fluorescein sodium salt, eosin Y and rose bengal) [27]. A mixed buffer solution of the photocurable gelatins and water-soluble difunctional macromers, which are PEGs end-capped with acrylate groups at both ends, was instantaneously converted to a water-swellable gel by UV or visible light irradiation. These photocurable gelatin-based materials have been used for tissue adhesive glues [28] or for regeneration scaffold materials [29,30]. When a saline solution of photoreactive gelatin alone was exposed to light, gel was formed with a yield of about 50%, but the generated gel was very fragile owing to a large degree of swelling of about 4. When a bifunctional macromer (PEG diacrylate with a molecular weight of about 4000) was added to this mixture, a strong and flexible gel with a degree of swelling of about 1 was obtained with a yield of about 90% under the same irradiation conditions. The rate of gel formation increased as the molecular weight of the macromer decreased. The produced gels contained an interpenetrating or interconnecting network that consisted of polymerized PEG and gelatin molecules and PEG-grafted gelatin. Gelatin is easily biodegraded and bioresorbed in body, whereas it is difficult to cleave the ether bonds that constitute PEG in the body, and therefore this degrade slowly.

In this study, we designed two series of novel poly(ether–ester)-based difunctional macromers to prepare biodegradable hydrogels, each of which had a well-defined number of ester bonds. Specifically, one series had a PEG central block extended with a chain of ester bonds, while the other had a repeating structure of oligo(ethylene glycol) blocks and two ester bonds. Both terminals of all poly(ether–ester)s were capped with acrylate groups and the total number of ester bonds in each macromer was precisely adjusted to range from 2 to 10. The introduction of degradable ester bonds in polyethers should lead to hydrolytic cleavage at these sites, which will lead to the production of low molecular weight polyethers that can be excreted in vivo. The photogelation characteristics of the poly(ether–ester) macromers and the mechanical properties and biodegradability of the produced hydrogels were also examined.

2. Materials and methods

2.1. General methods

All ^{1}H nuclear magnetics resonance (NMR) spectra were recorded in dimethyl sulfoxide (DMSO)–d_6 using tetramethylsilane (0 ppm) as an internal standard with a 270 MHz NMR spectrometer (JEOL, JNM-JX-270, Tokyo, Japan) at room temperature. All Fourier transform infrared (FT-IR) spectra were measured using a FTIR-8200A spectrometer (Shimadzu, Kyoto, Japan) by the KBr method. Gel permeation chromatography (GPC) analyses in dimethyl formamide were conducted with a Tosoh instrument (Tokyo, Japan), using Tosoh TSKgel α6000 and α3000 columns. The columns were calibrated with narrow weight distribution PEG standards.

2.2. Synthesis of PEG diacrylate (**1**)

A total of 2.5 g of dry PEG (M_w ~1000, ~2.5 mmol) was dissolved in 100 ml of 1,2-dichloroethane in a 200 ml round-bottomed flask and then cooled to 0 °C in an ice bath. A total of 1 ml of triethylamine and 0.905 g (10 mmol) of acryloyl chloride were added to the flask, and the mixture was then stirred for 12 h at 0 °C and 12 h at room temperature. The reaction mixture was filtered to remove triethylamine hydrochloride, after which PEG diacrylate (**1**) was obtained by pouring the filtrate into a large excess of dry diethyl ether. The mixture was further purified by dissolution and reprecipitation three times using 1,2-dichloroethane and hexane, respectively. Finally, the mixture was dried at room temperature under vacuum for 1 day. The yield of (**1**) was 2.69 g (97%). ^{1}H NMR (DMSO–d_6 with Me_4Si): δ 6.4 (2H, d,=CH_2), δ 6.2 (2H, dd, –C(C)H=CH_2), δ 6.0 (2H, d,=CH_2), δ 4.1 (4H, br, –CH_2–OCO–), δ 3.5 (84H, s, –O–CH_2–): FT-IR (KBr): 1735 cm^{-1} (–OCO–). The molecular weight was 1100 determined by GPC analysis and 1094 calculated by ^{1}H NMR.

2.3. Synthesis of PEG-based poly(ether–ester) macromer (**2**)

A total of 2.5 g of dry PEG (M_w ~1000, ~2.5 mmol) were dissolved in 100 ml 1,2-dichloroethane solution in a 500 ml round-bottomed flask and then cooled to 0 °C in an ice bath. A total of 1 ml of triethylamine and 7.75 g (50 mmol) of succinyl chloride in 100 ml of 1,2-dichloroethane were added to the flask, and the mixture was then stirred for 12 h at 0 °C and 12 h at room temperature. The reaction mixture was distilled to remove the unreacted succinyl chloride (70–75 °C/0.3 mm Hg). The residue was dissolved in 50 ml of 1,2-dichloroethane and then cooled to 0 °C. Next, 1 ml of triethylamine and 5.8 g (50 mmol) of 2-hydroxyethyl acrylate were added to the solution at 0 °C, and the mixture was then stirred for 12 h at 0 °C and 12 h at room temperature. After the solvent was removed, (**2**) was obtained with a yield of 61% by reverse-phase chromatography on silica gel (ethyl acetate/methanol = 1:1). ^{1}H NMR (DMSO–d_6 with Me_4Si): δ 6.3 (2H, d,=CH_2), δ 6.2 (2H, dd, –C(C)H=CH_2), δ 6.0 (2H, d,=CH_2), δ 4.3, 4.1 (12H, br, CH_2–OCO–), δ 3.5 (84H, s, –O–CH_2–), δ 2.5 (8H, br, –CH_2–COO–): FT-IR (KBr): 1734 cm^{-1} (–OCO–). The molecular weight was 1400 (GPC) and 1380 (NMR).

2.4. Synthesis of PEG-based poly(ether–ester) macromer (**3**)

The residue obtained after distillation of the reaction mixture of PEG (2.5 g, ~2.5 mmol, M_w ~1000) and succinyl chloride (7.75 g, 50 mmol) as described above was dissolved in 50 ml of 1,2-dichloroethane and then cooled to 0 °C. Next, 1 ml of triethylamine and 3.1 g (50 mmol) of ethylene glycol were added to the solution at 0 °C and the mixture was stirred for 12 h at 0 °C and 12 h at room temperature. After distillation to remove the unreacted ethylene glycol (55–60 °C/3 mm Hg), the residue obtained was dissolved in 50 ml of 1,2-dichloroethane at 0 °C. A total of 1 ml of triethylamine and 0.905 g (10 mmol) of acryloyl chloride was then added to this solution, after which the mixture was stirred for 12 h at 0 °C and 12 h at room temperature. The mixture was then filtered to remove

the triethylamine hydrochloride, after which the macromer (**3**) was obtained by pouring the filtrate into a large excess of dry diethyl ether. The product was further purified by dissolution and reprecipitation three times using 1,2-dichloroethane and hexane, respectively. Finally, the macromer was dried at room temperature under vacuum for 1 day. The yield of (**3**) was 1.41 g (33%). ^{1}H NMR (DMSO-d_6 with Me_4Si): δ 6.4 (2H, d,=CH_2), δ 6.2 (2H, dd, -C(C)H=CH_2), δ 6.0 (2H, d,=CH_2), δ 4.3, 4.1 (16H, br, -CH_2-OCO-), δ 3.5 (84H, s, -O-CH_2), δ 2.6 (16H, br, -CH_2-COO-): FT-IR (KBr): 1728 cm^{-1} (-OCO-). The molecular weight was 1700 (GPC) and 1670 (NMR).

2.5. Synthesis of penta(ethylene glycol)-based poly(ether–ester) macromer (*6*)

A mixture of penta(ethylene glycol) (3.03 g, 12.7 mmol) and succinic anhydride (3.78 g, 37.8 mmol) in 40 ml of pyridine was stirred at room temperature for 12 h, after which the reaction mixture was distilled to remove the pyridine (110–115 °C). The obtained residue was then washed with dilute hydrochloride solution and extracted with 1,2-dichloroethane. Next, the organic phase was washed with water, dried with Na_2SO_4, filtered and evaporated under vacuum. The yield of penta(ethylene glycol) ester derivative (**4a**) was 5.02 g (90%). ^{1}H NMR ($CDCl_3$ with Me_4Si): δ 4.27 (4H, COO-CH_2), δ 3.5–3.6 (16H, -OCH_2CH_2O-), δ 2.66 (8H, -OCO-CH_2-).

To a 1,2-dichloroethane solution (6 ml) of (**4a**) (1.76 g, 4.0 mmol) and penta(ethylene glycol) (9.5 g, 39.8 mmol) a 1,2-dichloroethane solution (2 ml) of 1,3-dicyclohexylcarbodiimide (DCC, 1.98 g 9.6 mmol) and *N,N*-dimethylaminoprydine (0.49 g, 4.0 mmol) was added at 0 °C. After stirring for 12 h at room temperature, penta(ethylene glycol) was removed by distillation (145–150 °C/0.3 mm Hg). The obtained residue was then purified by column chromatography on silica gel (elution with ethyl acetate/methanol = 1:1). The yield of the penta(ethylene glycol) ester derivative (**5a**) was 2.1 g (60%). ^{1}H NMR ($CDCl_3$ with Me_4Si): δ 4.25 (8H, COO-CH_2), δ **3.5–3.6** (52H, -OCH_2CH_2O-), δ 2.66 (8H, -OCO-CH_2-).

The obtained (**5a**) (2 g, 2.28 mmol) was mixed with acryloyl chloride (2.1 g, 22.8 mmol) and then stirred at 45 °C under a nitrogen atmosphere for 5 h. After distillation to remove the acryloyl chloride, the macromer (**6**) was obtained by pouring the filtrate into a large excess of dry diethyl ether. Finally, the macromer was dried at room temperature under vacuum for 1 day. The yield of (**6**) was 2.0 g (90%). ^{1}H NMR ($CDCl_3$ with Me_4Si): δ 4.30 (4H, CH_2=CH-COO-CH_2), δ 4.26 8H, COO-CH_2), δ 3.5–3.6 (48H, -OCH_2-CH_2O-), δ 2.66 (8H, -OCO-CH_2-). The molecular weight was 1000 (GPC) and 986 (NMR).

2.6. Synthesis of tri(ethylene glycol)-based poly(ether–ester) macromer (*8*)

Tri(ethylene glycol)-based Poly(ether–ester) macromer was prepared according to a similar procedure used to prepare (**6**). Tri(ethylene glycol) ester derivative (**4b**) was obtained by esterification of tri(ethylene glycol) (12.5 g, 83.2 mmol) by succinic anhydride (25 g, 250 mmol) in pyridine (40 ml). The yield of (**4b**) was 26.2 g (90%). ^{1}H NMR ($CDCl_3$ with Me_4Si): δ 4.28 (4H, COO-CH_2), δ 3.5–3.6 (4H, -OCH_2CH_2O-), δ 2.66 (4H, -OCO-CH_2-).

Tri(ethylene glycol) ester derivative (**5a**) was obtained by a condensation reaction of (**4b**) (4.32 g, 12.3 mmol) with tri(ethylene glycol) (18.6 g, 124 mmol) by DCC (6.1 g, 29.6 mmol) in 20 ml of 1,2-dichloroethane solution of 1,2-dimethylaminoprydine (1.52 g, 12.4 mmol). The yield of (**5b**) was 5.53 g (73%). ^{1}H NMR ($CDCl_3$ with Me_4Si): δ 4.28 (8H, COO-CH_2), δ 3.5–3.6 (28H, -OCH_2CH_2O-), δ 2.66 (8H, -OCO-CH_2-).

Tri(ethylene glycol) ester derivative (**7**) was obtained by repetition of two esterifications with succinic anhydride and then tri(ethylene glycol) as described above. The yield of (**7**) was 5.13 g (73%). ^{1}H NMR ($CDCl_3$ with Me_4Si): δ 4.25 (16H, COO-CH_2), δ 3.5–3.6 (44H, -OCH_2CH_2O-), δ 2.66 (16H, -OCO-CH_2-).

The macromer (**8**) was obtained by termination of (**7**) (2 g, 1.86 mmol) by acryloyl chloride (1.68 g, 18.5 mmol) as described above. The yield of (**8**) was 2.03 g (92%). ^{1}H NMR ($CDCl_3$ with Me_4Si): δ 4.28 (20H, -COO-CH_2-, CH_2=CH-COO-CH_2), δ 3.5–3.6 (40H, -OCH_2CH_2O-), δ 2.67 (16H, -OCO-CH_2-). The molecular weight was 1200 (GPC) and 1186 (NMR).

2.7. Photo-induced hydrogel preparation

A total of 30 mg of a bulk sample of the poly(ether–ester) macromers (99.5 wt.%) and camphorquinone (0.5 wt.%) (weight of the macromer content is W_{solid}), prepared by deaerating mixer (MX-201, THINKY Co.) for 5 min at 25 °C, was poured onto a circular glass coverslip (diameter 11 mm) and then photoirradiated with an argon ion laser (Spectra Physics argon ion laser Model Stabilite 2017 emitting at 488 nm) at a power density of 2 W cm^{-2} for the predetermined time. After thorough extraction with distilled water for (**1**), (**2**) and (**3**), or methanol for (**6**) and (**8**) to remove the non-reacted substances, the disk-shaped gels obtained were allowed to equilibrate with water overnight at room temperature, after which the excess water was carefully swabbed away and they were weighed (W_{water}). The vacuum-dried gels were also weighed (W_{gel}). The gel yield (%) was calculated as $W_{gel}/W_{solid} \times 100$. The degree of swelling (DS) was calculated as $DS = ((W_{water} - W_{gel})/W_{gel})$. The data of the gel yield and the degree of swelling were reproducible ($n = 5$, SD < 5%); therefore, only the average values are reported.

2.8. Mechanical studies

The measurements of both the tensile strength and the apparent elastic modulus of the gel prepared as described in the hydrogel preparation section were performed using a rheometer (RE-3305, Yamaden, Tokyo, Japan). The system was equipped with a 2 mm diameter rod-like Teflon probe and a sample stage with a 5 mm diameter hole at its center, and was able to measure the distance the probe runs to a gel as a function of the force applied.

Water-swelled disk-shaped gels were prepared by casting a bulk sample of the macromers (95.5 wt.%), including 0.5 wt.% of camphorquinone, on a circular glass coverslip (diameter 11 mm), followed by photoirradiation for 1 min similar to as described above. The gels were then washed, and immersed in distilled water overnight at room temperature. The total amounts of the samples were 20 mg for (**1**) and (**2**), 15 mg for (**3**), 40 mg for (**6**), and 50 mg for (**8**) to fix the hydrogel thickness of about 500 μm. The thickness was measured by a thickness meter attached to with the rheometer. The produced hydrogels were then placed at the center of the sample stage of the rheometer and force was applied until failure of the gels occurred by continuous loading of tension to the center of the gels using the probe at a cross-head speed of 0.5 mm s^{-1} in distilled water. The stress–strain curves were plotted by determining the stress as the load divided by the initial cross-sectional area strain in terms of the displacement divided by the initial length of the cylinder. Young's modulus was calculated as the slope of the initial linear portion of the stress–strain curves. The maximum stress value (P), defined as a tensile strength, was calculated as $P\,(Pa) = (A\,(g) \times 980)/(10 \times S\,(cm^2))$, where A and S denote the force value at gel rupture and contact area of the probe (0.031 cm^2), respectively. The apparent elastic modulus (E) of the gels was determined as $E\,(Pa) = P/(B\,(\%)/100)$ by extrapolating the linear fit of the deformation–force relationships obtained from the aforementioned tensile strength measurements, where B is

the development of the gel size expressed as the percentage volume modification with respect to the initial volume.

2.9. In vitro degradation

A 20 mg portion of each dry gel obtained according to the method as described in the hydrogel preparation section was used as a sample. The sample was immersed in 2 ml of phosphate-buffered saline (PBS) at pH 8.04. After shaking at 37 °C for predetermined periods, the reaction mixture was filtered (0.2 μm PTFE membrane filter, Toyo Roshi Kaisha Ltd., Tokyo, Japan) and then acidified to about pH 3 by adding a few drops of 6.0 N hydrochloric acid. The total organic carbon concentration (TOC) of the filtrate was measured using a TOC analyzer (TOC-10B, Shimadzu, Kyoto, Japan). The TOC values were the average of two measurements and were appropriately corrected by subtracting blank values.

2.10. In vivo evaluation

All animals received care according to the Principles of Laboratory Animal Care (National Institutes of Health, Publication No. 56-23, received 1985), and the research protocol (No. 9044) was approved by the ethics committee of the National Cerebral and Cardiovascular Center Research Institute.

Male Wistar rats (average weight 250 g) were used for all samples. The animals were anesthetized by intraperitoneal injection with pentobarbital sodium (50 mg/kg body wt) (Dainippon Pharmaceutical Co. Ltd., Osaka, Japan), after which the midportion of the back was shaved and sterile-prepped with isodine (Meiji Seika Kaisha Ltd., Tokyo, Japan). An incision (approximately 2 cm long) was made laterally on the dorsum using a surgical blade, after which subcutaneous pouches were made away from the incision using blunt scissors. Disk-shaped gels (30 mg), prepared as described above, were then inserted into each pouch, resulting in three specimens of the same formulation being implanted in each animal. The incisions were then closed with 3.0 ethilon suture (Ethicon, Somerville, NJ, USA).

The animals were killed at specific time points (1, 2 and 4 weeks) after surgery, after which the tissues adjacent to the gel samples were harvested using a surgical blade. For in vivo degradation analysis, all gels were removed from the tissue, washed with deionized water and then dried under vacuum for 1 day. Weight loss was monitored gravimetrically at various time intervals. For histological analysis, tissues surrounded the implanted gels were fixed with 10% formalin neutral buffer solution (pH 7.4) for at least 1 day. The tissues were then trimmed, dehydrated in a graded ethanol series, embedded in paraffin, and sectioned at a thickness of 4–5 μm with a microtome. After staining with hematoxylin and eosin, specimens were examined by light microscopy (Olympus AH-2 microscope, Tokyo, Japan).

3. Results and discussion

3.1. Preparation of poly(ether–ester) difunctional macromers

Two series of poly(ether–ester) difunctional macromers were molecularly designed. One series (**1**, **2** and **3**) contained a chain of several ester bonds at both ends of the central PEG block, and the other (**1**, **6** and **8**) had an alternating structure of oligo(ethylene glycol), each linked to ester bonds. The reaction procedures and chemical structure of the former series of the macromers are shown in Fig. 1. The former series, including three different PEG-based difunctional macromers, was prepared by stepwise chain extension reaction at both ends of the central PEG block to introduce a chain of several ester bonds and subsequent termination of acrylate groups. The molecular weight of the PEG block was adjusted to be about 1000. Macromer (**1**), which contains one ester bond at both ends of the PEG, was obtained by stirring the PEG in a large excess of acryloyl chloride. Macromer (**2**), which has three ester bonds at both ends of the PEG, was obtained by the esterification reaction of 2-hydroxyethyl acrylate and succinyl chloride-derivatized PEG at both ends. Monomer (**3**), which has five ester bonds at both ends of the PEG, was prepared by termination with 2-hydroxyethyl acrylate after two esterification reactions with succinyl chloride-derivatized PEG as obtained above and ethylene glycol and subsequent succinyl chloride. The chemical structures of the macromers were confirmed by ^{1}H NMR spectroscopy. The molecular weight of the macromers determined by GPC measurements and the total number of ester bonds per molecule were about 1100 and 2 in (**1**), about 1400 and 6 in (**2**), and about 1700 and 10 in (**3**), respectively (Table 1). These molecular weights were similar to those calculated from NMR data, indicating that both termini of all macromers were capped with acrylate groups. The macromers (**1**) and (**2**) were waxy solids, while (**3**) was viscous liquid at room temperature. All of these compounds were soluble in water.

Conversely, the latter series included three different types of difunctional macromers (**1**, **6** and **8**), consisting of a combination of an oligo(ethylene glycol) block and two ester bonds. The reaction procedures and chemical structures of the macromers are shown in Fig. 2. The macromers were prepared by several repetitions of esterification reactions of oligo(ethylene glycol) at both ends by succinic anhydride to obtain dicarboxylated oligo(ethylene glycol) and subsequent chain extension reaction with the same oligo(ethylene glycol) via condensation reaction by using of 1,3-dicyclohexycarbodiimide (DCC), except for the case of (**1**), which was used as a control in both series. Both terminal hydroxyl groups in both oligo(ethylene glycol) esters were converted to acrylate groups by a reaction with acryloyl chloride to obtain difunctional macromers. An oligomer, penta(ethylene glycol), and tri(ethylene glycol) were used in macromers (**6**) and (**8**), respectively. The total molecular weight of the macromers was about 1000 (by GPC) and 986 (by NMR) in (**6**), about 1200 (by GPC) and 1186 (by NMR) in (**8**) (Table 1) and the total number of ester bonds per molecule was 6 in (**6**) and 10 in (**8**). Both were viscous liquid at room temperature but insoluble in water. The water solubility of the poly(ether–ester)s with the alternating ether and ester bonds was lower than that of the former series of poly(ether–ester)s containing blocks of poly(ether)s and poly(ester)s.

3.2. Photogelation characteristics

The bulk of each poly(ether–ester) macromer (99.5 wt.%) mixed with a 0.5 wt.% of an initiator, camphorquinone, was exposed to visible light from an argon ion laser (488 nm, 2 W cm^{-2}). Within several tenths of a second of irradiation, water-swellable cross-linked three-dimensional gels had formed via free radical polymerization of the macromers, even in the presence of oxygen (Fig. 3). Additionally, the gel yield increased with irradiation time for all macromers. After 60 s of irradiation, almost all macromers were converted to gels with a high gel yield of approximately 80–90%, except for (**3**) (Table 1). A slight increase in the gel yield of (**3**) was observed even after prolongation of the irradiation time to over 60 s. The gel yield of (**3**) was under 70% even after 120 s of irradiation. Therefore, complete gelation reaching a plateau was obtained by 60 s of photoirradiation for all macromers except for (**3**). Regardless of the type of macromer, the degree of swelling of the gels decreases with the increase in gel yield, as shown for (**6**) in Fig. 3.

For the series of macromers (**1**), (**2**) and (**3**), a higher content of ester bonds, which was associated with a higher molecular weight,

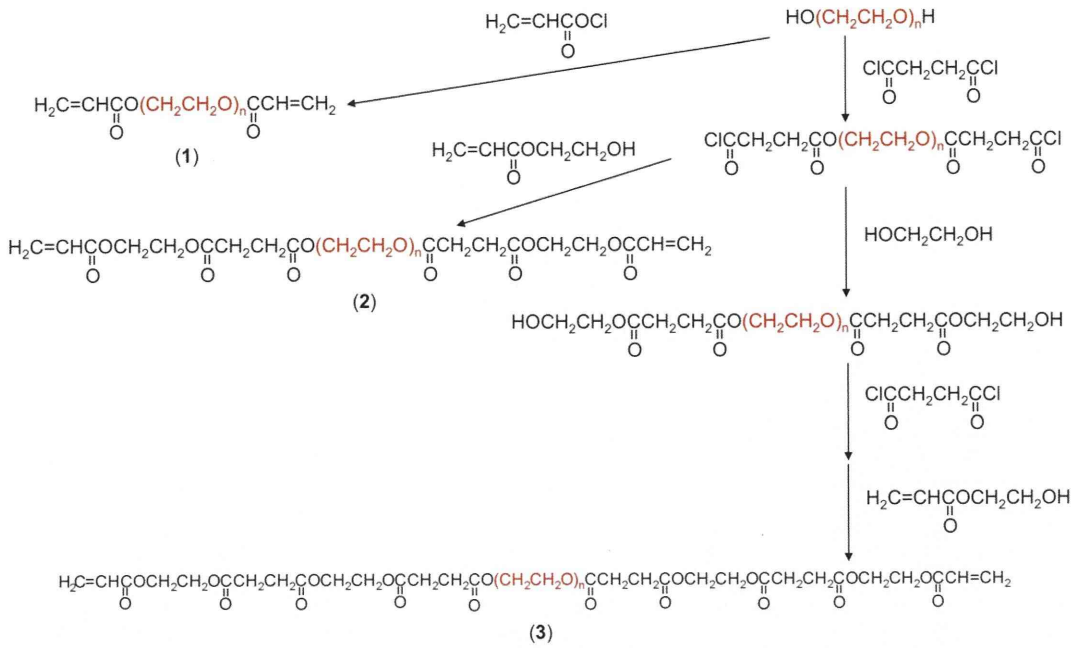

Fig. 1. Reaction scheme for the syntheses of three types of poly(ether–ester) macromers with a chain of 1, 3 or 5 ester bonds at both ends of the central poly(ethylene glycol) block and a molecular weight of about 1000.

Table 1
Characteristics and photogelation properties of the poly(ether–ester) macromers and the degree of swelling of the produced hydrogels.

Sample	M_n[a]	M_w[b]	Number of ester bonds in molecule	State at room temperature	Water solubility	Gel yield (%)	Degree of swelling
(1)	1100	1094	2	Wax solid	Soluble	89.1	1.6
(2)	1400	1382	6	Wax solid	Soluble	81.3	1.9
(3)	1700	1670	10	Viscous liquid	Soluble	64.6	4.0
(6)	1000	986	6	Viscous liquid	Insoluble	84.2	0.4
(8)	1200	1186	10	Viscous liquid	Insoluble	85.4	0.2

[a] Determined by GPC measurements.
[b] Calculated from ^{1}H NMR data.

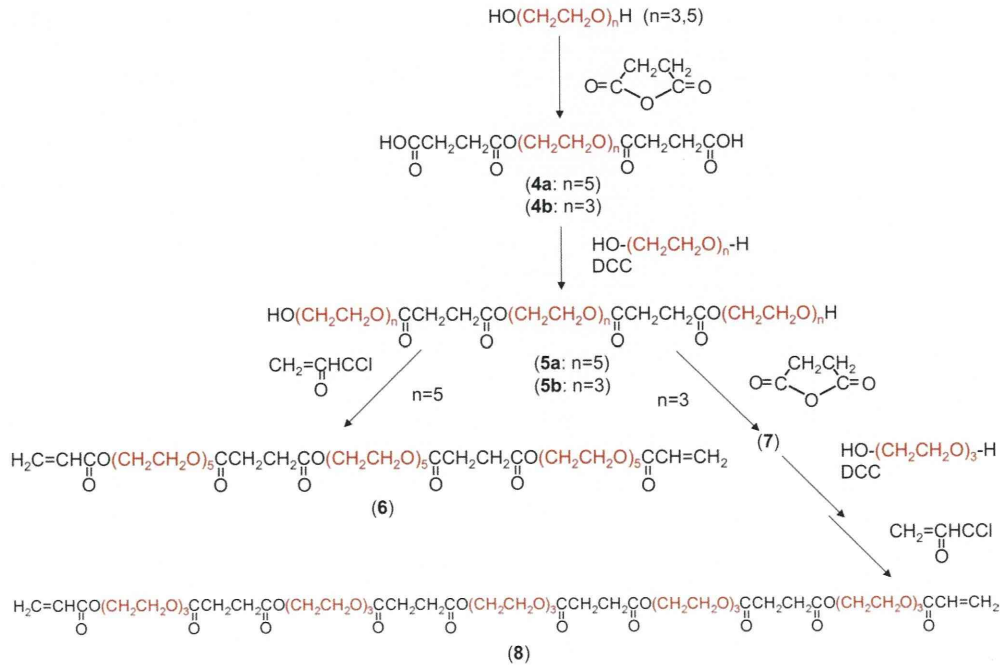

Fig. 2. Reaction scheme for the syntheses of three types of poly(ether–ester) macromers with an alternating structure of oligo(ethylene glycol), such as tri(ethylene glycol) or penta(ethylene glycol) blocks, and a couple of ester bonds, in which 6 or 10 ester bonds were incorporated equally on the macromers and the total molecular weight was adjusted to be about 1000.

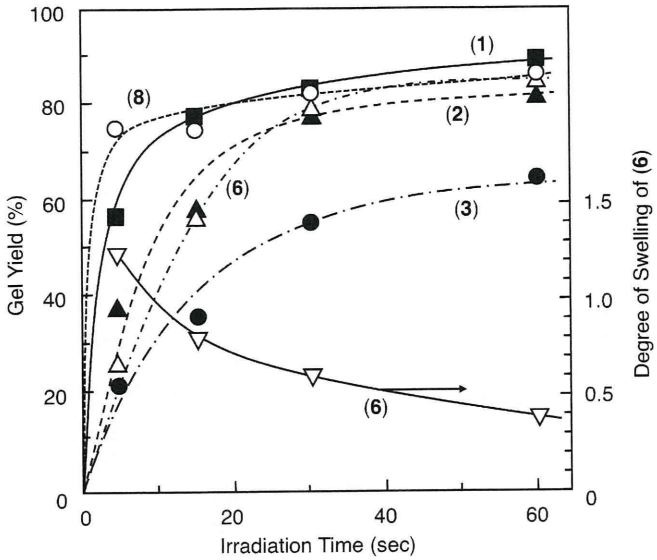

Fig. 3. Photogelation characteristics of the poly(ether–ester) macromers with 0.5 wt.% camphorquinone under different irradiation times and the degree of swelling of the gels produced from (**6**).

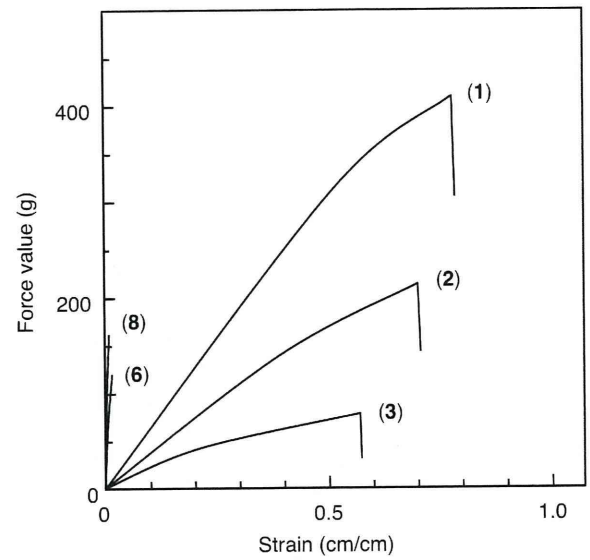

Fig. 4. Mechanical properties of the hydrogels produced from the poly(ether–ester) macromers (**1**), (**2**) and (**3**).

resulted in a lower gel yield and a higher water content (Table 1). The higher molecular weight macromers underwent a lower number of acrylate groups, which may have resulted in a lower gelation rate and a longer distance between cross-linking points. The different behavior in photogelation was observed especially for (**3**). This may be due to the difference in flexibility between poly(ester)s and poly(ether)s. Poly(ester) chains can affect each other via electrostatic interaction more strongly than can poly(ether) chains, which is reflected in the difference in the melting points. For example, the melting point of diethyl succinate is −20 °C and that of ethylene glycol diethyl ether is −74 °C. The high rigidity caused by extensive repetition of the ester bonding may prevent the terminal reactivity. A relatively low gel yield (about 70%) was reported in the photogelation of several poly(ester)s [20].

Conversely, there was little difference in gelation behaviors within the series of macromers (**1**), (**6**) and (**8**). The degree of swelling decreased as the number of ester bonds in the macromers increased, which was contrary to the former series.

3.3. Mechanical properties

The stress–strain relationships of the swollen gel films prepared by 1 min of photoirradiation of the bulk macromers with 0.5 wt.% camphorquinone are shown in Fig. 4. For the series of macromers (**1**), (**2**) and (**3**), gel rupture occurred under strains ranging from about 0.6 to 0.8. The calculated elastic modulus was 3.4×10^7 Pa in (**1**), 3.8×10^6 Pa in (**2**), and 1.6×10^6 Pa in (**3**).

Conversely, The gels from macromers (**6**) and (**8**) were ruptured at a strain just below the percentage of deformation (Fig. 4). Therefore, the elastic modulus of the gels was not determined exactly. These gels were hard, but extremely fragile.

3.4. Degradability

The photogelated macromers were subjected to in vitro hydrolysis. We used a TOC apparatus to evaluate the degree of in vitro degradation because TOC can precisely measure the carbon concentration of organic compounds eluted in water from the hydrogels on the ppm scale, and this technique has been established for several decades as a tool for measuring the degree of degradation of polymers [31,32]. By measurement of the filtrate from the hydrogel solution, the influence of fragmentation was excluded and a value for complete degradation could be measured.

Fig. 5 shows the degradation profiles of all of the swollen gels. Upon incubation in PBS solution at pH 8.04 and 37 °C, the gels were gradually converted into water-soluble products as the incubation period increased via fragmentation and the volume of the gels decreased, except for the gel from (**1**), which maintained its shape and underwent minimal degradation. The degradation rate was significantly enhanced as the content of ester bonds increased. In Fig. 5, a linear tendency in the degree of degradation was obtained after 1 week of incubation. Because the difference in the degradation property was clearly segregated by at least 3 weeks, we decided that this timescale was sufficient for the purposes of comparison. The amount of hydrolysis after 3 weeks of incubation was plotted as a function of the number of ester bonds per unit molecular weight (1000) in the macromers (Fig. 6). The degradation vol-

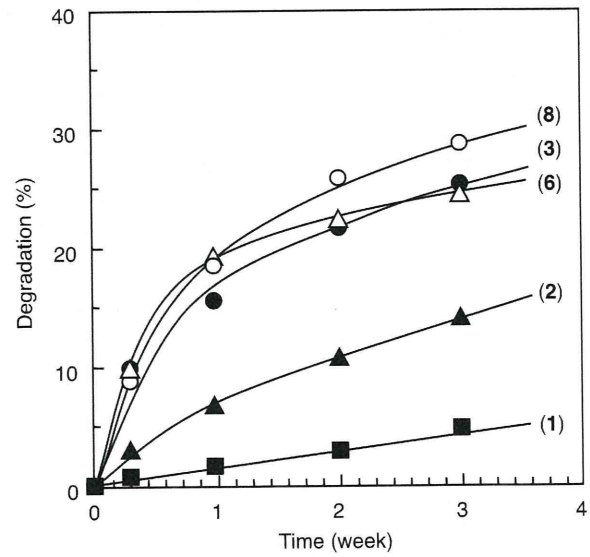

Fig. 5. Hydrolysis properties of the hydrogels produced from the poly(ether–ester) macromers at pH 8.04.

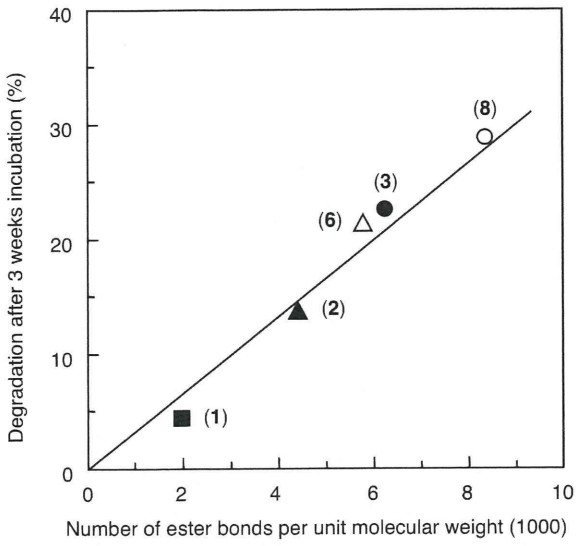

Fig. 6. Relationship between degradation of the hydrogels from the poly(ether–ester) macromers and the number of ester bonds per unit of molecular weight of 1000 in the macromers.

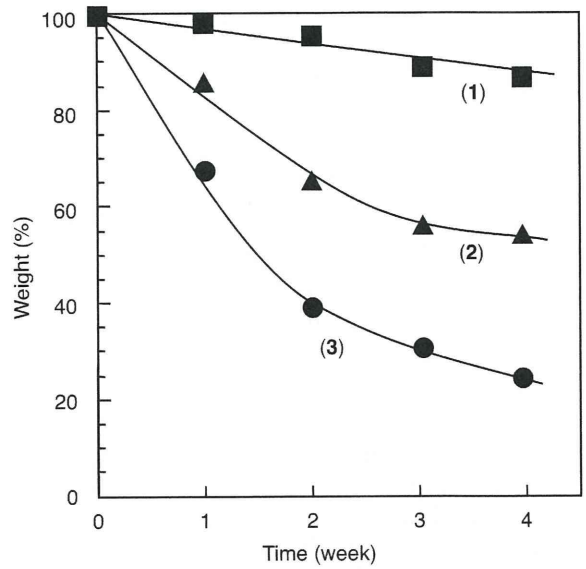

Fig. 8. In vivo degradation of the hydrogels produced from the poly(ether–ester) macromers.

ume linearly increased with an increase in the number of esters, regardless of the macromer structure.

The same degradation tendency was also observed in the in vivo study in which the materials were implanted in the rat subcutaneous pouches. One week after implantation, inflammatory cells were infiltrated from the tissue surrounding the hydrogel without signs of necrosis (Fig. 7). After 4 weeks the hydrogels were fully covered with collagenous encapsulation by connective tissues, in which little inflammatory cells were observed. There was little tissue migration into the hydrogels. There was no adhesion between the hydrogels and the surrounding tissues. Macroscopically, fragmentation and shrinkage of the hydrogels occurred via degradation in the collagenous capsule. This degradation might be induced mainly by hydrolysis. Therefore, the implanted hydrogels were easily removed from the formed capsular tissues even in the sample of macromer (**3**) after 4 weeks of implantation. On the other hand, because the hydrogels obtained from macromers (**6**) and (**8**) were hard, but extremely fragile, they were easily destroyed in the process of placing them into the subcutaneous pouches.

The in vivo degradation rate was determined by weight loss measurements (Fig. 8). The hydrogel prepared from macromer (**1**) underwent only a slight change in its weight. Conversely, the weight of the gels based on macromers (**2**) and (**3**) was markedly reduced as the implantation period increased. A higher content of ester bonds resulted in a higher susceptibility to degradation. After 1 month of implantation of the (**3**)-based gel, about 80% of its weight was lost.

4. Conclusion

We synthesized two series of novel PEG-based difunctional macromers by incorporating a precise number of ester bonds at both ends of the PEG chains. The gels prepared by photoirradiation showed accelerated degradation in proportion to the increase in

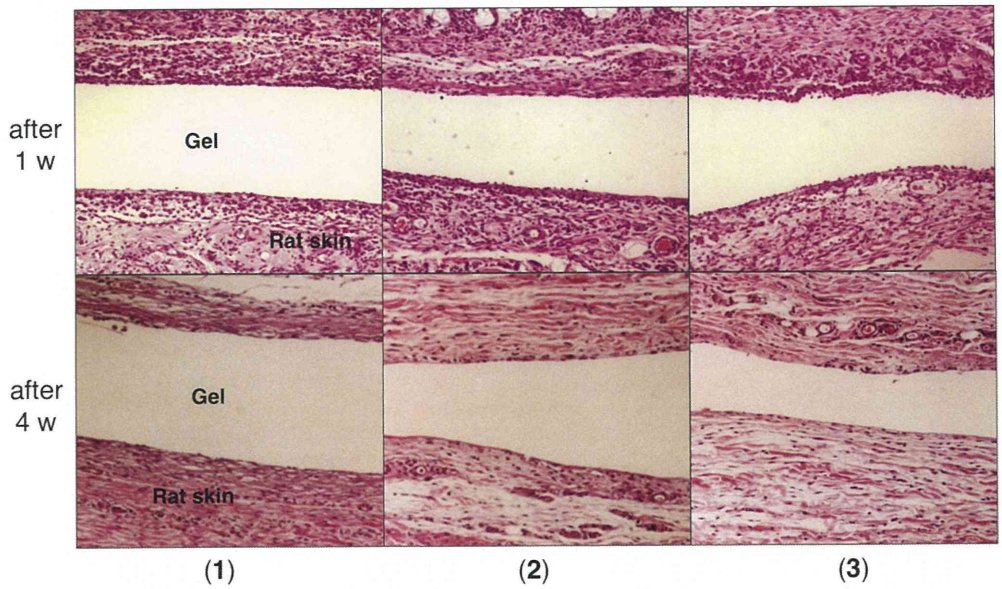

Fig. 7. Histological microphotos of rat skin after implantation of the hydrogels produced from the poly(ether–ester) macromers.

the number of ester bonds in the macromer molecule in vitro. The gels obtained from macromers with an alternating structure of oligo(ethylene glycol), each linked to two ester bonds, had unsatisfactory mechanical properties. On the other hand, the gels obtained from the macromers with a chain of ester bonds at both ends of the central PEG block had controllable mechanical and in vivo degradation properties. These PEG macromers may be useful for biodegradable biomaterials or tissue engineering scaffolds.

Appendix A. Figures with essential colour discrimination

Certain figures in this article, particularly Figures 1, 2 and 7, are difficult to interpret in black and white. The full colour images can be found in the on-line version, at doi:10.1016/j.actbio.2010.11.023.

References

[1] Van Tomme SR, Storm G, Hennink WE. In situ gelling hydrogels for pharmaceutical and biomedical applications. Int J Pharm 2008;355:1–18.
[2] Tabata Y. Biomaterial technology for tissue engineering applications. J Royal Soc Interface 2009;6(Suppl 3):S311–24.
[3] Corkhill PH, Hamilton CJ, Tighe BJ. Synthetic hydrogels. VI. Hydrogel composites as wound dressings and implant materials. Biomaterials 1989;10:3–10.
[4] Werker PM, Kon M. Review of facilitated approaches to vascular anastomosis surgery. Ann Thorac Surg 1997;63(6 Suppl):S122–7.
[5] Bawa P, Pillay V, Choonara YE, du Toit LC. Stimuli-responsive polymers and their applications in drug delivery. Biomed Mater 2009;4:022001.
[6] Pedrón S, Peinado C, Bosch P, Anseth KS. Synthesis and characterization of degradable bioconjugated hydrogels with hyperbranched multifunctional cross-linkers. Acta Biomater 2010 June 16 [Epub ahead of print].
[7] Zhang H, Zhao C, Cao H, Wang G, Song L, Niu G, et al. Hyperbranched poly(amine–ester) based hydrogels for controlled multi-drug release in combination chemotherapy. Biomaterials 2010;31:5445–54.
[8] Potta T, Chun C, Song SC. Chemically crosslinkable thermosensitive polyphosphazene gels as injectable materials for biomedical applications. Biomaterials 2009;30:6178–92.
[9] Zhu J. Bioactive modification of poly(ethylene glycol) hydrogels for tissue engineering. Biomaterials 2010;31:4639–56.
[10] Jevsevar S, Kunstelj M, Porekar VG. PEGylation of therapeutic proteins. Biotechnol J 2010;5:113–28.
[11] Lee DY, Park SJ, Lee S, Nam JH, Byun Y. Highly poly(ethylene) glycolylated islets improve long-term islet allograft survival without immunosuppressive medication. Tissue Eng 2007;13:2133–41.
[12] Yoshimoto T, Ritani A, Ohwada K, Takahashi K, Kodera Y, Matsushima A, et al. Polyethylene glycol derivative-modified cholesterol oxidase soluble and active in benzene. Biochem Biophys Res Commun 1987;148:876–82.
[13] Yamamoto Y, Tsutsumi Y, Yoshioka Y, Nishibata T, Kobayashi K, Okamoto T, et al. Site-specific PEGylation of a lysine-deficient TNF-alpha with full bioactivity. Nat Biotechnol 2003;21:546–52.
[14] Billinger M, Buddeberg F, Hubbell JA, Elbert DL, Schaffner T, Mettler D, et al. Polymer stent coating for prevention of neointimal hyperplasia. J Invasive Cardiol 2006;18:423–6.
[15] Nakayama Y, Miyamura M, Hirano Y, Goto K, Matsuda T. Preparation of poly(ethylene glycol)–polystyrene block copolymers using photochemistry of dithiocarbamate as a reduced cell-adhesive coating material. Biomaterials 1999;20:963–70.
[16] Drinnan CT, Zhang G, Alexander MA, Pulido AS, Suggs LJ. Multimodal release of transforming growth factor-beta1 and the BB isoform of platelet derived growth factor from PEGylated fibrin gels. J Control Release 2010 April 8 [Epub ahead of print].
[17] Vanderhooft JL, Mann BK, Prestwich GD. Synthesis and characterization of novel thiol-reactive poly(ethylene glycol) cross-linkers for extracellular-matrix-mimetic biomaterials. Biomacromolecules 2007;8:2883–9.
[18] Bettinger CJ, Bruggeman JP, Borenstein JT, Langer RS. Amino alcohol-based degradable poly(ester amide) elastomers. Biomaterials 2008;29:2315–25.
[19] Madhavan Nampoothiri K, Nair NR, John RP. An overview of the recent developments in polylactide (PLA) research. Bioresour Technol 2010 July 12 [Epub ahead of print].
[20] Grijpma DW, Hou Q, Feijen J. Preparation of biodegradable networks by photocrosslinking lactide, e-caprolactone and trimethylene carbonate-based oligomers functionalized with fumaric acid monoethyl ester. Biomaterials 2005;26:2795–802.
[21] Nottelet B, Pektok E, Mandracchia D, Tille JC, Walpoth B, Gurny R, et al. Factorial design optimization and in vivo feasibility of poly(epsilon-caprolactone)-micro- and nanofiber-based small diameter vascular grafts. J Biomed Mater Res A 2009;89:865–75.
[22] Sawhney AS, Pathak CP, van Rensburg JJ, Dunn RC, Hubbell JA. Optimization of photopolymerized bioerodible hydrogel properties for adhesion prevention. J Biomed Mater Res 1994;28:831–8.
[23] Elisseeff J, Anseth K, Langer R, Hrkach JS. Synthesis and characterization of photo-crosslinked polymers based on poly(L-lactic acid-co-L-aspartic acid). Macromolecules 1997;30:2182–4.
[24] Anseth KS, Shastri VR, Langer R. Photopolymerizable degradable polyanhydrides with osteocompatibility. Nat Biotechnol 1999;17:156–9.
[25] Kim BS, Hrkach JS, Langer R. Biodegradable photo-crosslinked poly(ether–ester) networks for lubricious coatings. Biomaterials 2000;21:259–65.
[26] Nguyen KT, West JL. Photopolymerizable hydrogels for tissue engineering applications. Biomaterials 2002;23:4307–14.
[27] Nakayama Y, Matsuda T. Photocurable surgical tissue adhesive glues composed of photoreactive gelatin and poly(ethylene glycol) diacrylate. J Biomed Mater Res 1999;48:511–21.
[28] Li C, Sajiki T, Nakayama Y, Fukui M, Matsuda T. Novel visible-light-induced photocurable tissue adhesive composed of multiply styrene-derivatized gelatin and poly(ethylene glycol) diacrylate. J Biomed Mater Res B: Appl Biomater 2003;66:439–46.
[29] Fukaya C, Nakayama Y, Murayama Y, Omata S, Ishikawa A, Hosaka Y, et al. Improvement of hydrogelation abilities and handling of photocurable gelatin-based crosslinking materials. J Biomed Mater Res B: Appl Biomater 2009;91:329–36.
[30] Hoshikawa A, Nakayama Y, Matsuda T, Oda H, Nakamura K, Mabuchi K. Encapsulation of chondrocytes in photopolymerizable styrenated gelatin for cartilage tissue engineering. Tissue Eng 2006;12:2333–41.
[31] Arvanitoyannis I, Nakayama A, Psomiadou E, Kawasaki N, Yamamoto N. Synthesis and degradability of a novel aliphatic polyester based on L-lactide and sorbitol: 3. Polymer 1996;37:651–60.
[32] Mochizuki M, Hirano M, Kanmuri Y, Kudo K, Tokiwa Y. Hydrolysis of polycaprolactone fibers by lipase – effects of draw ratio on enzymatic degradation. J Appl Polym Sci 1995;55:286–96.